INSTITUTE OF PHYSICS PUBLISHING JOURNAL OF PHYSICS B: ATOMIC, MOLECULAR AND OPTICAL PHYSICS

J. Phys. B: At. Mol. Opt. Phys. **35** (2002) R147–R193 PII: S0953-4075(02)89858-3

TOPICAL REVIEW

Atomic stabilization in superintense laser fields

Mihai Gavrila

Institute for Theoretical Atomic and Molecular Physics, Harvard-Smithsonian Center for Astrophysics, Cambridge, MA 02138, USA
and
FOM Institute for Atomic and Molecular Physics, Amsterdam, 1098 SJ, The Netherlands

Received 13 February 2002, in final form 19 July 2002
Published 9 September 2002
Online at stacks.iop.org/JPhysB/35/R147

Abstract

Atomic stabilization is a highlight of superintense laser–atom physics. A wealth of information has been gathered on it; established physical concepts have been revised in the process; points of contention have been debated. Recent technological breakthroughs are opening exciting perspectives of experimental study. With this in mind, we present a comprehensive overview of the phenomenon.

We discuss the two forms of atomic stabilization identified theoretically. The first one, 'quasistationary (adiabatic) stabilization' (QS), refers to the limiting case of plane-wave monochromatic radiation. QS characterizes the fact that ionization rates, as calculated from single-state Floquet theory, decrease with intensity (possibly in an oscillatory manner) at high values of the field. We present predictions for QS from various forms of Floquet theory: high frequency (that has led to its discovery and offers the best physical insight), complex scaling, Sturmian, radiative close coupling and R-matrix. These predictions all agree quantitatively, and high-accuracy numerical results have been obtained for hydrogen. Predictions from non-Floquet theories are also discussed. Thereafter, we analyse the physical origin of QS.

The alternative form of stabilization, 'dynamic stabilization' (DS), is presented next. This expresses the fact that the ionization probability at the end of a laser pulse of fixed shape and duration does not approach unity as the peak intensity is increased, but either starts decreasing with the intensity (possibly in an oscillatory manner), or flattens out at a value smaller than unity. We review the extensive research done on one-dimensional models, that has provided valuable insights into the phenomenon; two- and three-dimensional models are also considered. Full three-dimensional Coulomb calculations have encountered severe numerical handicaps in the past, and it is only recently that a comprehensive mapping of DS could be made for hydrogen. An adiabatic variation of the laser-pulse envelope keeps the system in the Floquet state associated with the initial state, that allows calculation of the ionization probability in terms of the corresponding rate. A nonadiabatic variation can excite other Floquet states, either discrete ('shake-up') or continuous ('shake-

off'), with considerable consequences for DS. A unitary interpretation of these aspects of DS is presented in terms of 'multistate Floquet theory'. We then comment on the points of contention raised in connection with DS. Further, we review the extent to which the classical approach has been successful in describing DS.

We next examine the concern that nonrelativistic (NR) predictions for stabilization may be inadequate in superintense fields, because relativistic corrections would invalidate them. It turns out that, although the relativistic corrections do limit stabilization, there is an ample 'window' of intensities for which the NR predictions remain valid.

Finally, we discuss the experimental evidence in favour of stabilization. For lack of adequate lasers to study ground states of single-active-electron atoms, the experiments so far have been performed on low-lying Rydberg states. Two state-of-the-art experiments have determined ionization yields for pulses with adiabatic envelopes. Their results concur, are in agreement with the theoretical predictions and represent a clear-cut confirmation of DS.

Our conclusion is that superintense field stabilization is firmly established, both theoretically and experimentally. Nevertheless, further research is desirable to solve interesting open problems, some of which we identify. Their research is made timely by the superintense high-frequency light sources that are being developed, such as VUV-FELs, or attosecond pulses from high-harmonic generation.

1. Introduction

An atom trapped in a superintense laser focus undergoes extreme contortion, which although ephemeral (subpicosecond duration) lasts long enough to allow for exotic manifestations. These could not be understood within the traditional perturbative framework, and new (nonperturbative) ideas had to be introduced. Considerable progress has thus been achieved, and a new goal for laser research has emerged in the process: instead of studying new behaviour of unperturbed atoms at low intensities, that of generating new atomic structure by means of the high intensities. Aside for its fundamental interest, this endeavour has interesting potential applications.

The exploration of intense laser–atom phenomena has been made possible by spectacular developments of laser technology. Focused laser pulses can now deliver superintense fields with peak electric amplitudes of up to 100 au, at wavelengths from the ultraviolet to the infrared, with high repetition rates. Already, at 1 au, the field amplitude is overwhelming: per definition, it equals the electric field of the proton on the first Bohr orbit of hydrogen. Pulse durations in the visible and infrared have now reached the level of several femtoseconds (a few cycles per pulse). In fact, the generation of superintense fields is coupled to that of short pulses, a combination that has proven ideal for the study of strong-field phenomena. Novel developments are actively pursued: high-frequency light sources delivering photons of several Rydberg energy, and attosecond pulses from high-harmonic generation.

A characteristic manifestation of intense field–atom interactions is *multiphoton ionization*. The range of the process has expanded over the years from the absorption of the minimal number of photons needed for ionization to that of hundreds of extra photons. In-depth studies of the properties of the ejected electrons (e.g. angular distributions, their response

to photon polarization) have been carried out. Gradually, interest has expanded from atoms with one active electron (hydrogen, alkali, noble gas atoms) to include those with two active electrons (helium, alkaline earth atoms), where the interplay of intense-field effects with electron correlation raises new problems.

The nonperturbative approach to multiphoton ionization has led to the discovery, a decade ago, of *'atomic stabilization'*, a fundamentally new concept. Lowest-order perturbation theory (LOPT) predicts multiphoton ionization rates that are steadily increasing with intensity I: for n-photon ionization, the rate grows as $\Gamma_n \sim I^n$. The growth appears to be quite natural: more driving force, more response. However, perturbation theory was apt to break down at some intensity. Whereas LOPT can be extended in principle to include higher-order corrections in the field, this turns out to be impractical. Direct nonperturbative handling of the Schrödinger equation is the right way to proceed. This led to a surprise, for it was found that the LOPT-predicted increase in ionization levels off at some intensity, and the reverse trend may set in: the higher the intensity, the lower the ionization. This, in general terms, is the *stabilization phenomenon*. The notion appeared as 'counter-intuitive', and so it is, from the perspective of perturbation theory. If one realizes, however, the profound changes the atom undergoes at high intensities, the puzzle disappears.

It should be noted that 'atomic stabilization', as described here, is one of several acceptations of this term. To fully characterize it, it should be qualified as 'superintense-field stabilization'. However, even in this context, terminology has been fuzzy at times and, as ideas progressed, occasionally turned out to be inadequate. We shall use in the following a terminology consistent with recent findings.

Superintense-field stabilization has emerged from both complementary approaches to the solution of the time-dependent Schrödinger equation (TDSE): the quasistationary approach and the wavepacket one. In the first case, wavefunctions are calculated for monochromatic, constant-amplitude fields, and ionization rates are derived. This has led to 'quasistationary stabilization' (QS), also known as 'adiabatic stabilization', which characterizes the globally decreasing *property of the rates* with respect to the field amplitude [1]. The second approach is the standard integration of TDSE to obtain wavepackets evolving from given initial conditions; it calculates *ionization probabilities* at the end of a laser pulse, expressing the *experimental ionization yields*. Beyond some large peak-field value of the laser pulse, these probabilities may manifest a behaviour that is globally decreasing, or plateau-like; this has been denoted 'dynamic stabilization' (DS) [2]. The connection between QS and DS was rather obscure in the beginning. It is only more recently that the two aspects could be integrated into a consistent, unitary picture, and some subtle issues have been clarified. While first discovered in quantum mechanics, stabilization was thereafter soon found to have a classical counterpart.

Among the numerous theoretical studies on stabilization published, the vast majority has confirmed the concept and has extended its realm. In recent years, however, criticism has emerged from two directions: numerical results disagreeing with mainstream calculations, and mathematical physics results, thought to be at variance with the physical ones. Many misunderstandings have meanwhile been cleared, leading to a better comprehension of the phenomenon[1].

The quantal description has been based on some *general assumptions* that we wish to state beforehand. Firstly, the radiation field is treated classically. This is justified by the fact that intense laser fields propagate extremely large numbers of photons, on the one hand, and, on the other, that we are interested here only in the motion of the electrons, rather than the

[1] The various points of view on atomic stabilization were presented at a panel discussion at *ICOMP 8 (Monterey, CA, 1999)*.

fact that they emit photons. Next, the dynamics are described nonrelativistically using the Schrödinger equation, because low electron velocities are involved in general. Finally, the dipole approximation (neglect of wave propagation within the atom) is used for the radiation field, which is acceptable for optical wavelengths and weakly perturbed atoms. The last two assumptions become questionable in superintense fields, and relativistic corrections need to be envisaged.

Computational limitations have been a perennial handicap in the theoretical study of the realistic three-dimensional (3D) case. In the early days of stabilization, they were quite severe even for the one-electron problem. This has encouraged studies of one-dimensional (1D) models, often termed 'numerical experiments'. Their merit is that, with reduced numerical gear, it was possible to study a large amount of cases, gaining valuable insight into the physics. However, quantitatively, their predictions can be misleading. In recent years the numerical difficulties have lessened, so that a comprehensive mapping of the 3D stabilization of H could be made.

Notwithstanding the great theoretical interest of stabilization, only two truly strong-field experiments have been done. Note that experiments in this area are extremely difficult, not to mention the high-tech equipment needed. These were carried out at FOM Amsterdam [3, 4], on low-lying Rydberg states, rather than ground states. This is because only for Rydberg states did the operational parameters of the available intense lasers satisfy the theoretical requirements for stabilization.

We list some general reviews on strong-field phenomena (in chronological order): Freeman *et al* [5, 6], Burnett *et al* [7], DiMauro and Agostini [8], Protopapas *et al* [9], Joachain *et al* [10]; for recent laser advances, see Brabec and Krausz [11], and also Mourou *et al* [12]. Reviews on superintense-field stabilization were presented by Gavrila [13], Eberly and Kulander [14], Delone and Krainov [15], Muller [16] and Gavrila [17][2]. Since these papers were written, important progress has been made in the quantitative description and physical understanding of the phenomenon. The goal of the present report is to cover this progress, while giving a comprehensive and unitary presentation of the physics. Issues related to ionization of high-lying Rydberg states are not covered here (for the latter, see Delone and Krainov [15], Lankhuijzen and Noordam [18] and Gallagher [19], and references therein).

The principal topics of our review are QS (section 2), DS (section 3), relativistic effects (section 4) and experiments (section 5), followed by a conclusion and perspectives (section 6).

We are using atomic units ($\hbar = m = |e| = 1$, where m and e are the mass and charge of the electron), unless otherwise stated[3].

2. Quasistationary stabilization

2.1. Floquet theories

2.1.1. Preliminaries. Assuming the dipole approximation, the electric field of a monochromatic plane wave can be written

$$\boldsymbol{E}(t) = E_0(\boldsymbol{e}_1 \cos \omega t + \boldsymbol{e}_2 \tan \delta \sin \omega t), \tag{1}$$

where E_0 is a real amplitude, $\boldsymbol{e}_1, \boldsymbol{e}_2$, are unit vectors orthogonal to each other and to the propagation direction and δ specifies the polarization; the averaged intensity of the wave is

[2] We take the oportunity of correcting two misprints in [17]: in equation (1), $\phi_n^{(v)}(\boldsymbol{r}, t)$ should read $\phi_n^{(v)}(\boldsymbol{r})$, and in equation (9) there should be a minus sign before the integral under the exponential.

[3] The values of some atomic units of interest here are in conventional units: length, 0.529×10^{-8} cm; time, 2.419×10^{-17} s; energy, 27.212 eV; electric field, 5.142×10^{9} V cm^{-1}; radiation intensity 3.509×10^{16} W cm^{-2} (defined as the time-averaged intensity of a linearly polarized field, with electric field amplitude of 1 au).

$I = E_0^2/\cos^2\delta$ au. The quiver motion of a classical electron in the laboratory frame, for an arbitrary field, is given in terms of the vector potential $\boldsymbol{A}(t)$ by

$$\boldsymbol{\alpha}(t) \equiv \frac{1}{c}\int_0^t \boldsymbol{A}(t')\,\mathrm{d}t'. \tag{2}$$

For the monochromatic plane wave equation (1) this gives $\boldsymbol{\alpha}(t) = (\alpha_0/E_0)\boldsymbol{E}(t)$, where $\alpha_0 \equiv E_0\omega^{-2}$ au.

We write for reference TDSE in the velocity gauge (laboratory frame):

$$\left[\frac{1}{2}\left(\boldsymbol{P} + \frac{1}{c}\boldsymbol{A}(t)\right)^2 + V(\boldsymbol{r})\right]\Psi = \mathrm{i}\frac{\partial\Psi}{\partial t}. \tag{3}$$

By applying a translation of vector $\boldsymbol{\alpha}(t)$ to the laboratory frame, one passes to the 'oscillating' or 'Kramers–Henneberger' frame, in which the classical electron is at rest. By also removing the 'quiver energy' term $(1/2c^2)\boldsymbol{A}^2$ via a phase factor transformation for convenience in equation (3), one finds the 'space-translated' TDSE:

$$\left[\frac{1}{2}\boldsymbol{P}^2 + V(\boldsymbol{r} + \boldsymbol{\alpha}(t))\right]\Psi = \mathrm{i}\frac{\partial\Psi}{\partial t}. \tag{4}$$

This contains the original potential $V(\boldsymbol{r})$ centred on the oscillating point $-\boldsymbol{\alpha}(t)$. It is unitarily equivalent to equation (3). The natural parameters describing the dynamics of an electron are now ω and α_0 (contained in $\boldsymbol{\alpha}(t)$, see equations (1), (2)), instead of the usual ω and E_0; ω and α_0 need to be regarded as independent parameters. Equation (4) was discovered by Pauli and Fierz [20], extensively used by Kramers (see [21, p 866]) and rediscovered by Henneberger [22], and also by Faisal [23][4].

Floquet theory[5] calculates quasistationary solutions of TDSE for a monochromatic field equation (1), of the form

$$\psi^{(\nu)}(\boldsymbol{r},t) = \mathrm{e}^{-\mathrm{i}E_\nu t}\sum_n \phi_n^{(\nu)}(\boldsymbol{r})\mathrm{e}^{-\mathrm{i}n\omega t}, \tag{5}$$

where E_ν is the 'quasienergy'. By requiring that $\psi^{(\nu)}$ satisfy TDSE, the Floquet components $\phi_n^{(\nu)}$ need to satisfy an infinite set of time-independent coupled differential equations. The system depends on the version of TDSE used (length or velocity gauge in the laboratory frame; space translated). Boundary conditions need to be imposed on the $\phi_n^{(\nu)}$ to ensure the uniqueness of the solution. To study ionization, these are mostly chosen of the Gamow–Siegert ('resonance-state') type, which leads to an eigenvalue problem with the quasienergy E_ν as eigenvalue. Because of the nature of these boundary conditions, E_ν is complex: $E_\nu \equiv W_\nu - (\mathrm{i}/2)\Gamma_\nu$. On the basis of qualitative arguments, the state ν is interpreted as representing an ionization mode of the atom, W_ν being the average energy in the field (modulo ω), and Γ_ν its ionization rate. The lifetime of the state is $\tau = 1/\Gamma$, in au. At vanishing field amplitude E_0, the Floquet system reduces to the unperturbed time-independent Schrödinger equation. Only one of the components $\phi_n^{(\nu)}$ survives, reducing to the unperturbed energy eigenfunction u_ν, while E_ν goes over into the corresponding field-free energy $W_\nu^{(0)}$.

Floquet theory based on using a single state equation (5), 'single-state Floquet theory', is the customary form of the theory, and will serve as a basis for discussion in this section. Although it has met with considerable success in describing multiphoton ionization, it has limitations stemming primarily from the fact that Floquet states are not square-integrable

[4] The quantized-field version of this equation, as used by Pauli and Fierz [20] and Kramers [21], has played a historical role in the development of the renormalization program of QED (see [24, chapter 7.4]).

[5] For various aspects of Floquet theory see Manakov *et al* [25], Chu [26], Potvliege and Shakeshaft [27], Burke *et al* [28], Joachain *et al* [10], Gavrila [13] and Moiseyev [29].

in the quantum mechanical sense, because of the Gamow–Siegert boundary conditions they satisfy. Moreover, Floquet solutions and their quasienergies imply constant field amplitude E_0, whereas intense laser fields are produced in the form of pulses. The issue is then how one can use single-state Floquet theory to describe physical reality. It turns out that this is possible for pulses with *adiabatically* varying envelopes $E_0(t)$, if the Floquet solution is known at all instantaneous values of the amplitude $E_0(t)$ during the pulse (and therefore the time dependence of the quasienergy $E_\nu[E_0(t)]$). For arbitrary pulses, superpositions of Floquet states need to be considered. These issues will be discussed in section 3.2.

Concerning the practical determination of Floquet states, a variety of methods has been applied successfully: complex scaling (or complex coordinate rotation), Sturmian basis expansion, radiative close coupling, R-matrix Floquet (see, e.g., [9]). However, the physics of stabilization derives naturally from the 'high-frequency Floquet theory' (HFFT), which has also made the discovery of the phenomenon possible.

2.1.2. High-frequency Floquet theory. HFFT is a general framework for treating laser–atom interactions at high frequencies and all intensities (see Gavrila and Kaminski [30], for an overview see [13]), which proceeds from the space-translated Schrödinger equation (4). HFFT solves the corresponding Floquet system of equations at large ω by successive iterations of increasing order in ω^{-1} [13]. To lowest order in ω^{-1} (the high-frequency limit) and at fixed α_0, the HFFT Floquet system reduces to a single equation, the *'structure equation'*:

$$[\tfrac{1}{2}\boldsymbol{P}^2 + V_0(\alpha_0, \boldsymbol{r})]v_\nu = W_\nu v_\nu, \tag{6}$$

and the Floquet state $\psi^{(\nu)}(\boldsymbol{r},t; E_0, \omega)$ of equation (1) reduces to $\psi^{(\nu)} \simeq \mathrm{e}^{-\mathrm{i}W_\nu t}\, v_\nu(\boldsymbol{r})$. Equation (6) has the form of a usual energy-eigenvalue Schrödinger equation containing the 'dressed potential' $V_0(\alpha_0, \boldsymbol{r})$, defined as the time average of the oscillating potential:

$$V_0(\alpha_0, \boldsymbol{r}) \equiv \frac{1}{T}\int_o^T V(\boldsymbol{r} + \boldsymbol{\alpha}(t))\,\mathrm{d}t, \tag{7}$$

where $T = 2\pi/\omega$. Thus, in the high-frequency limit the quasienergies are real, $\lim \mathrm{Re}\, E_\nu = W_\nu$ and $\lim \Gamma_\nu = 0$, which means that ionization is frozen. Moreover, the equation contains only α_0 (but not ω), and hence $W_\nu = W_\nu(\alpha_0)$. The $v_\nu(\boldsymbol{r}; \alpha_0)$ will be referred to as 'dressed eigenfunctions'.

The structure equation (equation (6)) was first obtained heuristically by Henneberger [22], but its high-frequency character was recognized only later by Gersten and Mittleman [31]; ionization, and hence QS, were not considered in these papers. In the context of HFFT, equation (6) was first derived for radiation-assisted scattering [30].

The occurrence of V_0 in equation (6) appears natural if one notes that the nucleus has an oscillatory motion of trajectory $-\boldsymbol{\alpha}(t)$ in the oscillating frame. As ω is supposed large, the electron will not react to the rapid oscillations of the nuclear potential, but rather to its time average V_0 (see [13, section IV C]). Equivalently, equation (7) can be expressed as a line integral along the ellipse $-\boldsymbol{\alpha}(t)$, with variable charge density (higher at the points where the motion is slower), so that V_0 can be regarded as the electrostatic potential obtained by smearing out the nuclear charge along its trajectory. This 'line of charge' reduces to a segment of length $2\alpha_0$ for linear polarization (with higher density towards its end points $\pm\alpha_0\boldsymbol{e}$, where $\boldsymbol{e}$ is the polarization vector), or a circle of radius α_0 in the polarization plane, for circular polarization (with constant charge density) (see [13, section IV C]). As opposed to the original Coulomb potential, the dressed potential has in general only a logarithmic singularity along the line of charge. For linear polarization, however, it has extra square-root singularities at the end points $\pm\alpha_0 e$. A graphical representation of the dressed potential for the linear case was given by Gavrila and Kaminski [30, figure 1], and for the circular case by Pont [32, figure 1].

The first iteration within the HFFT allows for *ionization*. For the partial n-photon ionization rates this gives [33]

$$\frac{d\Gamma_n}{d\Omega} = k_n |f_n(\hat{\boldsymbol{k}})|^2, \qquad f_n(\hat{\boldsymbol{k}}) \equiv -\frac{1}{2\pi}\langle v_{\boldsymbol{k}_n}^{(-)}|V_n|v_0\rangle, \tag{8}$$

where we have dropped the state label ν. Here $\boldsymbol{k}_n$ is the final momentum of the electron [$\boldsymbol{k}_n \equiv k_n\hat{\boldsymbol{k}}$; $(k_n^2/2) = W_\mu + n\omega$] and v_0, $v_{\boldsymbol{k}_n}^{(-)}$, are respectively the initial and final dressed states of the electron, adequately normalized (v_0 having normalization integral equal to unity, and $v_{\boldsymbol{k}_n}^{(-)}$ having asymptotic amplitude unity). Angular integration of equation (8) gives the n-photon ionization rate Γ_n, and Γ is obtained from $\Gamma = \sum_n \Gamma_n$. The rates depend on both ω and α_0 (or E_0). The first iteration also yields a correction to the real part of the quasienergy, i.e. a correction of $\mathcal{O}(1/\omega)$ to the dressed energy levels W_ν of equation (6), which substantially improves the agreement with the the exact Floquet value (see Marinescu and Gavrila [34]). Explicit formulae for the second iteration were given by Wells *et al* [35]. In the following, we shall limit ourselves to results from the first iteration.

A pragmatic convergence criterion for the HFFT iteration scheme was shown to be the *high-frequency condition* [13]:

$$\omega \gg W_{exc}(\alpha_0), \tag{9}$$

where $W_{exc}(\alpha_0)$ is an average excitation energy for the manifold of the initial state v_0. For linear and circular polarizations, the manifolds are characterized by parity, and the magnetic quantum number m. Most often, $W_{exc}(\alpha_0)$ is of the order of magnitude of the largest binding energy of the manifold. Equation (9) requires that at least one-photon ionization be possible. Equation (9) is a sufficient condition, and HFFT results may apply even when it is not satisfied. There are *no* restrictions on α_0 in HFFT[6]. Mathematical aspects of HFFT were discussed by Martin and Sassoli de Bianchi [36].

The structure equation (6) was first solved for the case of hydrogen, and posed a numerical challenge because of its nonseparable character. A variety of methods have been applied, with the result that the eigenvalues and eigenfunctions of H and other simple systems (H^-, H_2^+) are known to a high degree of accuracy (see Pont *et al* [37, 38] and Pont [32], and also [13])[7]. We display in figure 1 $W(\alpha_0)$ for the ground state of H as a function of $I^{1/2}\omega^{-2}$ au, cases of linear and circular polarizations. (Note that, when α_0 is expressed in terms of I, we have $\alpha_0^{(lin)} = I^{1/2}\omega^{-2}$ and $\alpha_0^{(circ)} = (I/2)^{1/2}\omega^{-2}$ au.) The figure shows that, if the high-frequency condition (9) is satisfied at all intensities, the binding energy of the atomic ground state in the field *decreases steadily to zero*. Coupled to this decrease are peculiar changes in the atomic structure. For linear polarization the electronic cloud elongates and undergoes 'dichotomy' into two nonoverlapping lobes, localized around the end points $\pm\alpha_0\boldsymbol{e}$ of the line of charge [37, figure 1], [38, figures 5, 6], [13, section VB and figures 4, 5]. For circular polarization, the cloud concentrates in a torus around the circle of charge of radius α_0 ('toroidal shaping') [32], [13, section VB and figure 6]. Note that these structural changes occur in the oscillating frame, and are perceived differently in the laboratory frame.

Solutions of the structure equation (equation (6)) have since also been derived for 1D systems with various short-range potentials, which are easier to handle numerically than

[6] The condition $\alpha_0^2\omega \gg 1$, mentioned by Gavrila and Kaminski [30], and reproduced in the reviews [7, 9, equation (8.5)], has turned out to be superfluous.

[7] The numerical methods applied were diagonalization in multicentre Gaussian basis sets (Pont *et al* [37, 38]), two independent finite element programs (Vos and Gavrila [39], Shertzer *et al* [40]) and diagonalization in a Slater-type basis set in spheroidal coordinates (Muller and Gavrila [41]). More recently, Lefebvre and collaborators have shown that it is possible to solve equation (6) to good accuracy, by applying efficient quantum chemistry codes, such as HONDO 95.6 (see Perez *et al* [42]).

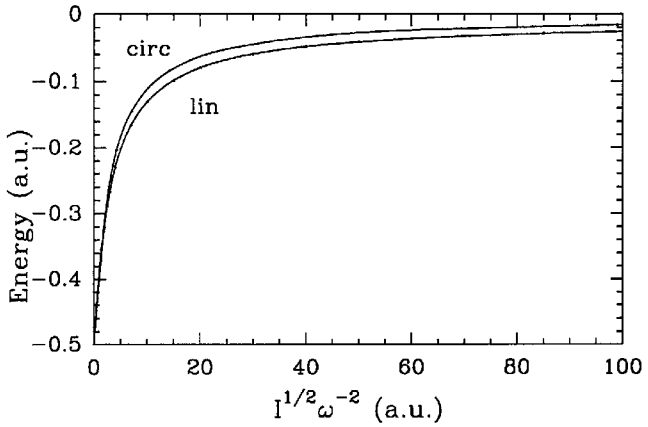

Figure 1. Ground-state energy of the H atom in high-frequency laser fields (linear and circular polarizations) versus $\alpha_0 = I^{1/2}\omega^{-2}$ (in au), according to the HFFT (from Pont *et al* [38] and Vos and Gavrila (unpublished)).

Coulomb-tail potentials. The case of the attractive Gaussian potential was worked out by Bardsley and Comella [43], Yao and Chu [44] and Marinescu and Gavrila [34]. The 'zero-range' potential $V(x) = -B\delta(x)$ was treated partly analytically by Grozdanov *et al* [45]; see also Sanpera *et al* [46]. A characteristic of short-range 1D potentials (with a finite number of field-free bound states) is that the system acquires additional bound states as the field increases. These have been designated 'light-induced states' (LIS), and exist also for the full Floquet differential system. For the structure equation (equation (6)), as α_0 varies, new LIS bound states materialize from resonance states. This was illustrated by Boca *et al* [47] for the $\delta(x)$ potential. There is a substantial difference between the 1D and 3D cases concerning LIS for short-range potentials, as discussed by Potvliege [48]: pending reasonable conditions on the potential, in the 1D case the number of LIS increases indefinitely for $\alpha_0 \to \infty$, whereas in the 3D case it tends to zero[8,9].

Solutions of the structure equation (equation (6)) for 1D long-range potential models have also been derived, especially for the 'soft-core Coulomb' potential (see section 3.1.1).

The fact that Floquet quasienergies should depend only on α_0 in the high-frequency limit appeared to be puzzling at first, but was soon confirmed by full Floquet computations. Bardsley and Comella [43] have shown, using their Gauss-potential 1D model, the progressive approach of Re $E(\alpha_0, \omega)$ towards the HFFT value $W(\alpha_0)$ as ω increases; see also Ben-Tal *et al* [49]. A detailed comparison of full Floquet calculations with the complete form of the first iteration of HFFT was carried out by Marinescu and Gavrila [34] for the same Gauss potential. For H, the approach of Re $E(\alpha_0, \omega)$ towards $W(\alpha_0)$ was confirmed by Dörr *et al* [50, 27] (see also section 2.1.2). The behaviour of Floquet functions, at high and low frequencies, was compared during a light period, by Wiedemann [51] for a 1D 'soft-core' Coulomb potential,

[8] For more information on LIS, see also Fearnside *et al* [52], and references therein. Their physical reality was ascertained on the basis of TDSE wavepacket calculations by Wells *et al* [53].

[9] Interest in 3D short-range potential models stems from the fact that they give an adequate representation for the behaviour of negative ions (like H^-) at low intensities. However, it follows from [64, 41, 65] that at high intensities, one-particle models for the description of H^- completely break down (see also the end of section 2.1.2), and a two-particle description is needed. As an illustration, we recall that H^- acquires an increasing number of bound states in superintense fields [64, 41], whereas the models tend to lose all their bound states [48].

$V_s(x) = -(1+x^2)^{-1/2}$: in the former case the modulus of the function is nearly constant in time, as predicted by HFFT, whereas in the latter case it undergoes strong oscillations.

The calculation of rates for H according to equation (8) was done by Pont and Gavrila [1] (see also [13, section VI]). Beside the ground-state wavefunction v_0 one needs the continuum function $v^{(-)}_{\boldsymbol{k}_n}$. The simplest approximation for the latter is the Born approximation (replacement of $v^{(-)}_{\boldsymbol{k}_n}$ by a plane wave). This greatly simplifies the calculation and allows for the derivation of analytic formulae capable of illustrating the physical trends. On the other hand, it limits the validity of the results to larger values of ω than those required by the high-frequency condition of the theory (see [34]).

For circular polarization, the results can be obtained analytically, and for the ground state of H we find

$$\frac{\mathrm{d}\Gamma_n}{\mathrm{d}\Omega} \simeq \frac{4}{k_n^3}[v_0^{(c)}]^2 J_n^2(\alpha_0 k_n \sin\theta), \qquad \Gamma_n \simeq \frac{8\pi}{\alpha_0 k_n^4}[v_0^{(c)}]^2 \int_0^{2\alpha_0 k_n} J_{2n}(\xi)\,\mathrm{d}\xi. \tag{10}$$

Here, J_n is a Bessel function, θ is the angle of $\boldsymbol{k}_n$ with the propagation direction of the field and $v_0^{(c)}$ is the constant value (due to cylindrical symmetry) of the ground-state wavefunction v_0 on the 'circle of charge'.

At low intensities (small α_0) equation (10) gives $\Gamma_1 \sim I$, with an ω dependence of $\omega^{-9/2}$; this is a well known result from LOPT at high frequencies. Moreover, as $\Gamma_n \sim I^n$, to lowest order in the intensity only Γ_1 contributes to the total rate Γ: $\Gamma \simeq \Gamma_1 \sim I$.

For intense, nonpertutbative fields ($\alpha_0 k_n \gg 1$), Γ_n of equation (10) can be summed analytically over n. If also $\alpha_0 \gg 1$, one finds that $v_0^{(c)} \simeq (0.147/\alpha_0)$, which yields the dominant behaviour:

$$\Gamma \simeq \frac{0.223}{\alpha_0^3\,\omega^2} = 0.631\frac{\omega^4}{I^{3/2}}, \qquad (\alpha_0 \gg 1). \tag{11}$$

This equation exhibits the 'QS' phenomenon: *at fixed* ω the total ionization rate decreases with I; at fixed I, Γ increases with ω. An alternative designation is *'adiabatic stabilization'*[10]. More generally, we shall define QS, allowing for an *overall* decreasing behaviour of Γ at high intensities (not necessarily monotonic).

QS exists also for general elliptic polarization. For linear polarization, the dominant high-frequency behaviour at large α_0 was derived by Pont and Gavrila (see [13, section VI.2]):

$$\Gamma \simeq \frac{\omega^2}{I}\left(0.007\,46\ln\frac{I}{\omega} + 0.285\right), \qquad (\alpha_0 \gg 1). \tag{12}$$

This approximates the accurate Floquet results of [50, figure 3] to better than 20% at $\alpha_0 > 1$. On the other hand, equation (11) is considerably less accurate, which indicates a larger magnitude of the neglected terms (see [50, figure 5]).

The intensity dependence of the lifetime τ of H for circular polarization, as computed from equation (10), is shown in figure 2 at various ω. For the larger ω ($1 \leqslant \omega \leqslant 8$), condition (9) is (approximately) satisfied, so that it is meaningful to follow the HFFT lifetimes from small intensities to superintensities. In the log–log plot shown, a lifetime curve has three branches: a linearly descending branch at low intensities (slope approximately minus one) representing LOPT, followed by an intermediate branch with a minimum and then by the quasi-linearly ascending QS branch (slope roughly 3/2, see equation (11)). At very high α_0, the results shown will be affected by as yet unknown relativistic corrections. The vague oscillatory

[10] 'Adiabatic stabilization' is a term introduced early on (1993) to characterize the fact that one is dealing with the stabilization of rates Γ derived from Floquet theory, the practical realization of which implies adiabaticity. However, to avoid confusion with *dynamical stabilization* of the ionization probability P_{ion} occurring under adiabatic conditions of variation of the pulse envelope (see section 3.2), we henceforth give preference to the term 'QS'.

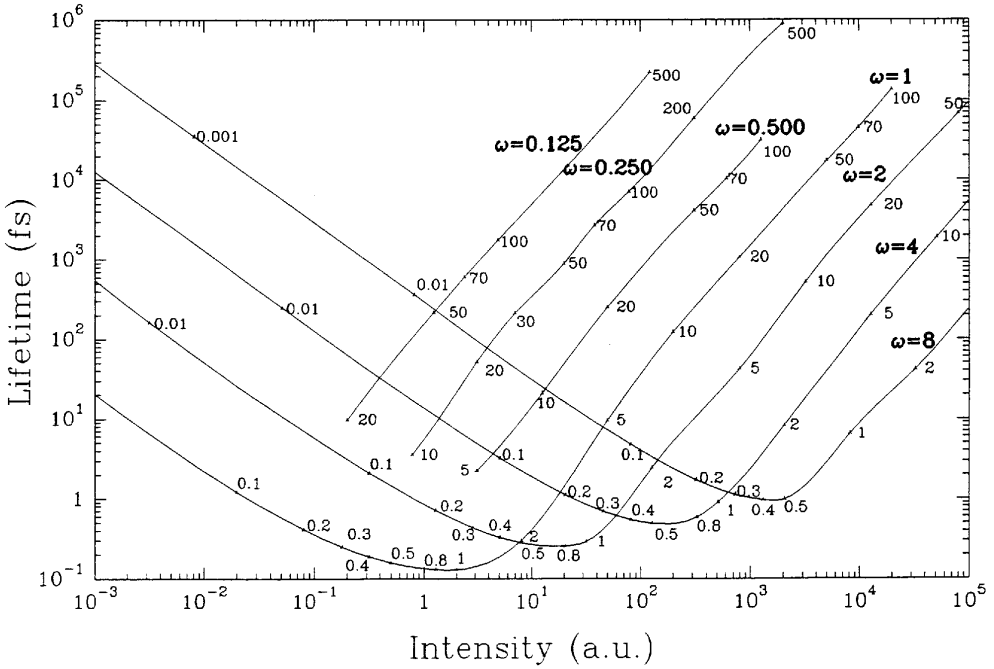

Figure 2. Lifetime of the H atom in the ground state according to the HFFT, versus intensity, at various ω (in au); circular polarization. Numbers adjacent to points on the curves are the corresponding values of α_0. The descending branches of the curves correspond to LOPT, the ascending ones to QS (from Pont and Gavrila [1]).

behaviour of the stabilization branches in figure 2 can be traced back to the Bessel function oscillations of $(\mathrm{d}\Gamma_n/\mathrm{d}\Omega)$, equation (10). However, these oscillations practically wash out, when integrating over the angles and summing over n, to calculate the total rate Γ.

Also included in figure 2 are three τ curves at lower ω ($\omega = 0.125, 0.25, 0.5$), which have not been continued towards small intensities. This is because the high-frequency condition (9) is violated at small intensities, where the binding energy is approximately 0.5, and therefore the ground-state solution of equation (6) cannot be considered physical. Nevertheless, due to the decrease in the binding energy (and of E_{exc}) illustrated in figure 1, at sufficiently high I, the high-frequency condition ends up by being satisfied. When this happens, the ground-state solution becomes physical according to the HFFT, and the curves in figure 1 do represent its lifetimes. This is an example of LIS, states generated by the radiation field.

Lefebvre *et al* [54] have carried out a computation of the ionization rates according to equation (8), without making the Born approximation for the final state $v_{\boldsymbol{k}_n}^{(-)}$ (but still not fully accurate, however). This improves substantially the agreement of equation (8) at $\alpha_0 < 1$ with the accurate Floquet computations by Dörr *et al* [50, 55] (see section 2.1.3). The fact was confirmed subsequently by Lefebvre and Stern [56]. The same conclusion was drawn from the 1D model calculation in [34].

It was recognized from the very beginning of QS studies that the experimental means to demonstrate its existence for the ground state of atomic H were not available (lack of high-frequency lasers and the required intensities). Besides, the laser pulses need to be sufficiently short, otherwise the atom would not be able to survive the rising edge of the pulse in a neutral state, and enter the stabilization regime: it would ionize while crossing the valley-shaped

branch of its lifetime curve in figure 2, which acts like a 'death valley' (see section 3.1[11]). Nevertheless, it was realized by Vos and Gavrila [39] that it should be possible to detect QS with the existing experimental means for Rydberg states.

The advantage of considering *Rydberg states* is that, even for small ω, by choosing a sufficiently high-lying state, its binding energy will be smaller than ω, so that condition (9) would appear to be satisfied. The difficulty is that there could be lower-lying states coupled to the initial state, leading in fact to a W_{exc} larger than ω. The way out proposed in [39] was to use a linearly polarized field, since the HFFT states can now be grouped into noninteracting manifolds characterized by the magnetic quantum number m with respect to the field axis (the strict selection rule $\Delta m = 0$ holds). Thus, equation (9) can be written as $\omega \gg W_{exc}^{(m)}$, where $W_{exc}^{(m)}$ is the average excitation energy for the manifold of the initial state, and is of the order of magnitude of the excitation energy of its lowest state. The lowest state of quantum number m is a 'circular state' with $|m| = l = n-1$; its field-free binding energy is $W^{(m)}(0) = 2^{-1}(|m|+1)^{-2}$. By choosing m high enough, $W_{exc}^{(m)} \simeq W^{(m)}(0)$ can be made small with respect to any of the frequencies ω of available intense lasers. As it turns out that for $\alpha_0 > 0$, $W^{(m)}(\alpha_0) < W^{(m)}(0)$ (see [39, figure 1], or [13, figure 3]), the high-frequency condition is even better satisfied as the intensity increases. Besides, a H-atom calculation will suffice, as high atomic states are essentially hydrogenic. Similar ideas were advanced by Pont and Shakeshaft [59].

The calculation in [39] focused on the two lowest-lying dressed states of the $|m| = 5$ manifold. The odd state of the manifold goes over in the field-free limit into $n = 6$, $l = 5$, whereas the even state goes into $n = 7$, $l = 6$. The eigenfunctions were calculated quite accurately first, using equation (6); very good agreement with these results was found later in [60]. Ionization was then calculated at $\omega = 1.17$ eV $= 0.0428$ au, and $\omega = 2.0$ eV $= 0.0735$ au (the latter photon energy being that of the experiments described in section 4), both satisfying the condition $\omega \gg W_{exc}^{(m)}$. The two curves obtained for the lifetimes τ are similar in shape to those in figure 2 for the ground state, with the essential difference that for the circular Rydberg states the minimal lifetimes exceeded by far the duration of the intense short laser pulses available at that time (some 100 fs), and hence 'death valley' was no longer lethal for the neutral atom. It was concluded (1992) that all conditions were satisfied in the cases considered to be able to detect QS with the available technological means. Moreover, it turned out that, due to the Born approximation made for the final dressed state, the lifetimes were severely underestimated, so that the situation was even more favourable for an experiment. This was shown by Potvliege and Smith [61] and Baik *et al* [60] (see further, sections 2.1.3 and 2.2).

There are also other differences between QS for Rydberg states and the ground state: the onset of QS occurs for the Rydberg states at lower intensities (below 0.1 au), and the stabilization branch increases more steeply with I. Moreover, the total lifetime for high-m states of principal quantum number n is determined entirely by one-photon ionization, i.e. $\Gamma \simeq \Gamma_1$, for it was predicted in [39] to be $\Gamma_n \sim n^{-|m|-2}(n \geqslant 1)$. This means that practically only one-photon ionization occurs, and that there is only one peak in the electron spectrum.

Let us now address the natural question *what is the physical origin of QS?* Several, not so obviously equivalent, interpretations have been advanced (e.g. Pont and Shakeshaft [59], Potvliege and Smith [61] and Scrinzi *et al* [62]). These have led to the conclusion that the value for the onset of QS is $\alpha_0^{(m)} \sim \omega^{-1/2}$. We present here the interpretation emerging from our HFFT formulae.

[11] The fact that atoms would not survive in a neutral state to feel the peak intensities of picosecond pulses was emphasized much earlier by Lambropoulos [58].

Recall that ionization is described quantum mechanically by de Broglie probability waves emitted by the oscillating electron in the presence of the nucleus. In the oscillating frame of reference, it is the nucleus that moves along the trajectory $-\boldsymbol{\alpha}(t)$. Let us consider the asymptotic form of the Floquet component $\phi_n(\boldsymbol{r})$, describing n-photon ionization, in the Born approximation:

$$\phi_n(\boldsymbol{r})_{v\to\infty} \to \frac{f_n e^{ik_n r}}{r} \simeq -(2\pi)^2 \overline{V}(\boldsymbol{k}_n)\frac{1}{T}\int_0^T e^{in\omega t}\frac{e^{ik_n|\boldsymbol{r}+\boldsymbol{\alpha}(t)|}}{|\boldsymbol{r}+\boldsymbol{\alpha}(t)|} v_0[-\boldsymbol{\alpha}(t)]\,dt. \tag{13}$$

Here, $\overline{V}(\boldsymbol{k})$ is the Fourier transform of the field-free potential $V(\boldsymbol{r})$, and $v_0[-\boldsymbol{\alpha}(t)]$ is the initial dressed eigenfunction at the trajectory of the nucleus[12]. Equation (13) contains two independent parameters, α_0 and $\alpha_0 k_n \sim \alpha_0\omega^{1/2}$. The emitted wave $\phi_n(\boldsymbol{r})$ appears as a superposition of instantaneous emissions taking place at each point of the trajectory, weighted by the local magnitude of the electronic wavefunction $v_0[-\boldsymbol{\alpha}(t)]$. The total emission in a given direction will be subject to interference. The elements controlling ionization are thus de Broglie *interference* and the amount of *electronic presence* along the path of the nucleus, $v_0[-\boldsymbol{\alpha}(t)]$. If the linear size of the trajectory (of order α_0) is smaller than the emitted wavelength, i.e. $\alpha_0 k_n \lesssim 1$, there can be only constructive interference. Since this implies small α_0, and $v_0[-\boldsymbol{\alpha}(t)]$ is then nearly constant (it has approximately the value of the unperturbed eigenfunction at the origin $u(0)$), $|f_n|$ will increase with α_0. This trend is stopped by *two* causes. (a) Destructive interference occurring when the emitted wavelength becomes smaller than the linear size of the trajectory, i.e. $\alpha_0 k_n > 1$. This decrease leads to an interference minimum which, as in optics, will be followed by a maximum, and so on; the amplitudes of the successive maxima decrease, however, with their order, and hence with α_0. (b) Weakening of the electronic weight function $v_0[-\boldsymbol{\alpha}(t)]$. This is a consequence of the fact that the dressed potential becomes progressively weaker as α_0 increases (for details see [13]), which makes the eigenfunction expand, and $v_0[-\boldsymbol{\alpha}(t)]$ be a decreasing function of α_0. The decrease with α_0 of $|f_n|$, occurring in all directions, leads to a decrease of the angle-integrated Γ_n for all n, and of their sum Γ. (In fact, at high frequencies, the dominant contribution comes from Γ_1 at all α_0.) Causes (a) and (b) are both responsible for QS, and neither of them can be considered separately. Whereas (b) has a classical analogue, (a) does not (see section 3.4).

The effects of the two causes can be simply illustrated for circular polarization. In this case, $v_0[-\boldsymbol{\alpha}(t)] \equiv v_0^{(c)}$ is constant along the circle of charge, and factors out of the integral in equation (13). The latter then yields a Bessel function (see equation (10)), with asymptotic amplitude $\sim\alpha_0^{-1/2}$; this is responsible for the interference phenomenon. On the other hand, $v_0^{(c)}$ is a decreasing function at all α_0 (at large α_0, $v_0^{(c)} \sim \alpha_0^{-1}$), which is a consequence of the expansion of the wavefunction with α_0. In the expression of Γ_n, equation (10), at larger α_0 (in the QS range), $[v_0^{(c)}]^2$ contributes a factor α_0^{-2}, whereas the square of the Bessel function contributes a factor α_0^{-1}. Were $v[-\boldsymbol{\alpha}(t)]$ in equation (13) to be constant, all Γ_n and Γ would be functions of $\alpha_0\omega^{1/2}$ only, and the onset of QS would occur at some $\alpha_0^{(m)}$ such that $\alpha_0^{(m)}\omega^{1/2} =$ constant, as predicted in [61]. The fact that cause (b) is also operative makes the onset of QS depend also on α_0; this lowers the value of[13] $\alpha_0^{(m)}$.

[12] Equation (13) originates in equation (82) of [13], with $\nu = 1$ (first iteration). The latter equation contains $\Omega_n^{(1)} = V_n$ (see equations (72) and (73)); further, for consistency to first order, we set $\phi_0^{(1)} \simeq \phi_0^{(0)} = v_0$, $G(E_n^{(1)}) \simeq G^{(+)}(W_n)$ (see [13, p 465]). For $G^{(+)}(W_n)$ we then take the Born approximation, and use for V_n its defining Fourier integral. This leads to our equation (13), if the slowly varying function $v_0[\boldsymbol{r} - \boldsymbol{\alpha}(t)]$ is handled as described in [13, p 489]. Note that f_n resulting from equation (13) is consistent with the Born approximation of f_n in equation (8).

[13] Note that QS is not due to the 'dichotomy' (for linear polarization), or the 'toroidal shaping' (for circular polarization) of the electronic cloud, as was sometimes stated, because these effects appear for ground-state H at much larger α_0 (e.g. $\alpha_0 \gtrsim 30$) than the onset of stabilization ($\alpha_0 \approx 1$).

Equation (13) is a useful approximation as long as $v_0[-\boldsymbol{\alpha}(t)]$ is nonvanishing. For linear polarization, the line of charge is located on the field axis, and v_0 is nonvanishing only if it belongs to the $m = 0$ manifold (containing the ground state); v_0 vanishes on the field axis for states with $m \neq 0$. In this case the interpretation of QS cannot be based on equation (13). Nevertheless, we have given a generalization of equation (13) to the case $m \neq 0$, which has a similar form, except that $\overline{V}(\boldsymbol{k}_n)$ is replaced by a derivative with respect to the momentum variables $\boldsymbol{k}_n$, and v_0 by a spatial derivative at points located on the line of charge. This allows the interpretation of QS to be carried out as for $m = 0$ states.

We have dealt so far with HFFT for one-electron atoms. The theory has been generalized, however, to *several-particle HFFT*, and applied to two-electron atoms, simple molecules and exotic systems. For two-electron atoms, one obtains the space-translated Schrödinger equation by translation of the coordinates of each electron by $\boldsymbol{\alpha}(t)$, equation (2). Note that the Coulomb repulsion energy retains its form. Subsequent application of the high-frequency iteration procedure leads to the following structure equation:

$$\left[\frac{1}{2}(\boldsymbol{P}_1^2 + \boldsymbol{P}_2^2) + V_0(\alpha_0, \boldsymbol{r}_1) + V_0(\alpha_0, \boldsymbol{r}_2) + \frac{1}{|\boldsymbol{r}_1 - \boldsymbol{r}_2|}\right] v_\nu = W_\mu v_\nu, \tag{14}$$

and to a generalization of equation (8) for the differential single-electron ionization rates (see [64]). Equation (14) treats the two electrons on the same footing. Consequently, it is natural that the validity condition be given by equation (9), where now W_{exc} is the average excitation energy for the whole system. At small intensity, W_{exc} can be relatively high (e.g., for H^- it is of the order of the binding energy for H), but at high intensity this can be very much reduced (see [63, 64]). We recall that equation (9) is a sufficiency condition.

Equation (14) was applied to the calculation of the structure of H^-, with full account of electron correlation, by Muller and Gavrila [41]. Whereas in the field-free case H^- has only one bound state, at increasing intensities it acquires a large (probably infinite) set of LIS. The large-α_0 behaviour of the system was investigated by Mittleman [63] for the ground state, and by Gavrila and Shertzer [64] for all states. It was found that the total binding energy of H^- becomes *twice* that of H [63], and that, of the large number of LIS that appear, some are doubly excited but not subject to autodetachment [64]. QS was confirmed only at large α_0 [64]. Using the Born approximation, it was found that, in the dichotomy regime, the H^- ionization rate is essentially *twice* that of H. In fact, QS is expected to set in at much smaller α_0, but the issue was not investigated quantitatively.

Exotic atomic structures have been predicted at large α_0, from the several-electron form of equation (14), by van Duijn *et al* [65] and van Duijn and Muller [66]. For example, it was shown that a proton can bind three or more electrons (i.e., multiple negative ions of H can exist) in monochromatic, or specially chosen bichromatic high-frequency fields, a fact not possible in the field-free case. The production of H^{2-} (one proton plus three electrons) should be within experimental reach. As, at large α_0, the electrons involved are practically independent dynamically, the single-electron decay rates of these systems are proportional to the corresponding hydrogen decay rates, and the ions are in the QS regime already at appearance.

2.1.3. Other Floquet theories. QS has been confirmed for the ground state and the excited states of H, in fields of linear or circular polarization, by all other Floquet theories: Sturmian, radiative close coupling, R-matrix Floquet and complex scaling. The Floquet differential systems solved derive either from the Schrödinger equation in the laboratory frame, or from its space-translated version. These theories obtain directly the complex quasienergies, and hence the average atomic energy W (modulo ω) and the total Γ. The latter depend in general both on α_0 and ω. Extra effort is needed to determine the partial rates Γ_n.

Explicit Floquet *results for* $W(\alpha_0, \omega)$ at finite ω were reported for the case of H only by Dörr *et al* [50, figure 1], see also [27, figure 18], at a number of frequencies, for linear and circular polarizations. In both cases the field-dependent Stark shift for the ground state is positive and increases (i.e., the *binding energy decreases*), as predicted by HFFT (see figure 1). By increasing ω, one could follow the approach of $W(\alpha_0, \omega)$ towards the HFFT value $W(\alpha_0)$ in figure 1. For both polarizations, at lower α_0, we have $W(\alpha_0, \omega) < W(\alpha_0)$, whereas at higher α_0, $W(\alpha_0, \omega) > W(\alpha_0)$. For $\alpha_0 \gtrsim 4.5$ the agreement with $W(\alpha_0)$ becomes close at all frequencies $\omega > 0.51$.

The *results for* Γ in the QS regime are as follows.

Sturmian theory [27, 67]. Dörr *et al* [50] have obtained accurate results for QS of the 1s and 2s states of H, for linear and circular polarizations, with ω in the range $0.51 < \omega < 2$. The Floquet system solved was that corresponding to the Schrödinger equation in the velocity gauge. Γ curves were obtained as functions of α_0. For the 1s state, Γ_{1s} starts from zero at $\alpha_0 = 0$, passes a maximum (corresponding to the bottom of the 'death valley' for the lifetime) and decreases thereafter to zero (QS regime). QS is present already at ω as low as 0.51, and at fixed α_0 the values of Γ_{1s} decrease with increasing ω, as expected from HFFT. Up to some α_0 in the range 2–4, $\Gamma_{1s}^{circ} > \Gamma_{1s}^{lin}$, but thereafter the situation is reversed, in agreement with the high-α_0 HFFT predictions (see equations (11) and (12)). A similar behaviour of the Γ curves was found for the 2s state at various frequencies. At given ω, Γ_{2s} is about one-tenth of Γ_{1s}. Note that QS was found to exist even at $\omega = 0.17$ and 0.25, energies that do not satisfy the high-frequency condition (9). This indicates that condition (9) is sufficient, but not necessary.

Potvliege and Smith [61] have applied Sturmian theory to Rydberg states of high m quantum number, for several wavelengths ranging from the visible to the infrared, and linear polarization. QS was demonstrated in all cases, and a table was made of intensities for the onset of QS in these states, and the corresponding values of the lifetimes. A comparison with the results of Vos and Gavrila [39] showed that, although the Γ curves had similar shapes, there were large discrepancies in their magnitudes (due to the use of the Born approximation in [39]). Potvliege [68] has also considered QS for Rydberg states in a two-colour field, consisting of a superposition of the first and second harmonic of $\omega = 2$ eV with variable amplitude ratio and phase difference (linear polarization). The presence of the second harmonic affects QS significantly only at very high amplitude ratio, contrary to what happens in the 1D case [57].

R-matrix Floquet theory [10, 28, 69] solves for each problem the Floquet system in different gauges, depending on the region of configuration space considered, and then connects the solutions at the boundaries. Intended for several-electron atoms, it was applied to hydrogen as a test case by Dörr *et al* [55] (1s and 2s states, linear polarization). The ω chosen for the 1s state ($\omega = 0.65$) was (marginally) a high frequency in the sense of equation (9); that for the 2s case ($\omega = 0.184$) was a low frequency. QS was found in both cases, in excellent agreement with the Sturmian results of [50]. Partial rates have also been obtained.

Radiative close-coupling theory in the angular momentum basis [70, 71] was applied by Dimou and Faisal [72] to solve the Floquet system corresponding to the space-translated Schrödinger equation (equation (4)) and circular polarization. QS for the 1s and 2s states of H was confirmed, the results being in good agreement with those of the Sturmian theory [50] for the 1s state; for the 2s state they were calculated at different frequencies. A subsequent paper [73] treated the case of Rydberg states and linear polarization, at frequencies satisfying the high-frequency condition (9). A table of critical intensities for the onset of QS, together with the corresponding values of Γ, was presented for several states. In general, the results were in good agreement with those of [61].

Marte and Zoller [74] have solved the radiative close-coupling equations to obtain the scattering matrix $S(E)$ at positive energy, and parametrized it with the help of the multichannel

quantum defect theory (MQDT). This makes the analytic continuation of $S(E)$ possible below the $n\omega$ thresholds, where its poles, representing the quasienergies of the resonances, can be determined. Γ obtained for the 1s state at one ω was in fair agreement with [50].

More recently, Lefebvre and Stern [56] have applied the radiative close-coupling method using exterior scaling for the solution of the radial differential equations. The Floquet system solved was that corresponding to equation (4). The Γ obtained for the 1s state at $\omega = 5$, 10, 20, 50 manifests QS in all cases, as well as the partial rates Γ_n. As ω increases, Γ_1 approaches Γ, as predicted by HFFT (since $\Gamma_n \sim 1/n^2$).

Complex scaling theory [26, 29]. The Floquet Hamiltonian was chosen either in laboratory frame forms (in the coordinate, or momentum representations), or in the oscillating frame form. Early 1D calculations are those by Bardsley and Comella (see [43], and references therein), and Yao and Chu [44]. The latter have shown that, for the Gauss-potential model considered, Γ is not a monotonically decreasing function of the intensity in the stabilization regime, but presents oscillations described by Bessel functions. This was confirmed by subsequent 1D calculations [75, 76, 34], etc. As noted above, this type of behaviour also occurs for the differential angular rate of H (see e.g. equation (10)), but there it gets washed out by the integration over the angles, when obtaining Γ.

For H, Zakrzewski and Delande [77] have determined the quasienergies of the 2p, $m = 0, \pm 1$ states in circularly polarized light with $\omega = 0.25$, in order to study the connection of QS and DS (see the discussion in section 3.2). Buchleitner and Delande [78] have discussed the ionization and stabilization of high-lying Rydberg states, the emphasis lying on behaviour in microwave fields. Their method is equivalent to the Sturmian method of Dörr *et al* [50], with which it gave good agreement. Scrinzi *et al* [62] have also focused on higher Rydberg states with $l = 0$, $m = 0$ (linear polarization). The ω chosen were in some cases larger than the initial binding energies of the Rydberg states considered, but they did not satisfy the high-frequency condition (9), as ω was small in comparison with the average excitation energy of the $m = 0$ manifold, which is $W_{exc}^{(0)} \simeq 0.5$ (see the discussion in section 2.1.2 in connection with $W_{exc}^{(m)}$). Nevertheless, their Γ curves did exhibit QS regimes, in some cases Γ having a single maximum, like that of the ground state (see their figure 1), in other cases having several maxima (their figure 4).

To conclude our survey of Floquet results for Γ, we note that the values for H agree rather well with each other, and in some cases excellently, which is quite gratifying in view of the diversity of the methods used. In comparison with the HFFT results, numerical Floquet theories can claim greater accuracy, because they integrate the exact form of the Floquet system, and hence are equivalent to including higher-order corrections in ω^{-1} to the HFFT equations we have used. Besides, no approximation is made concerning the ionized electron. It has also emerged that QS can exist, even when the high-frequency condition (9) is not satisfied, although the circumstances under which this happens have not been investigated.

2.2. Non-Floquet theories

Quasienergies can be obtained by a variety of methods, without solving the Floquet system of differential equations. We are presenting some that have been used in the study stabilization.

We consider first the case of 3D models with 'zero-range potentials', potentials acting over an infinitesimal range around a centre that have been applied to the description of negative ions. These remarkable models can be solved analytically at all field strengths. They have been considered in various forms, depending on the way the coupling to the field was introduced. One choice is the '$\delta(\boldsymbol{r})$ potential' model, with $V(\boldsymbol{r}) = C\delta(\boldsymbol{r})\partial(r\ldots)/\partial r$, coupled to a monochromatic circularly polarized plane wave. It was solved by Berson [79] and Manakov

and Rapoport [80] using the *Green function* (see also Faisal *et al* [81], Krstic *et al* [82], and, for linear polarization, Filipowicz *et al* [83]). Quasienergies are determined from a complicated transcendental equation, and the differential n-photon ionization rates can be obtained independently in terms of Bessel functions. The evaluation of Γ (from the transcendental equation, or from summation of the n-photon rates) is a delicate mathematical and numerical issue, and has led to contradictory statements on stabilization. Thus, LaGattuta [84] obtained numerical results for Γ based on S-matrix theory, showing QS in the range of ω and E_0 considered. Krainov and Preobrazhenskii [85], on the other hand, asserted the total absence of stabilization, but Manakov *et al* [86] disputed their result, finding numerically that Γ did decrease up to a certain field, increasing thereafter. Kaminski [87] proved the inexistence of stabilization within the HFFT at asymptotically high intensities. He also discussed the difference in behaviour of 3D and 1D zero-range models, since the latter does exhibit stabilization, as shown in section 2.1.2. Although mathematically interesting, zero-range potentials are artificial constructions, that do not shed light on the stabilization of systems with usual potentials. Besides, being one-particle models, they are unrepresentative for negative ions at high intensities (see section 2.1.2 and footnote 9).

A method based on *analytic continuation* in the field amplitude E_0 was devised by Baik *et al* [60]. The idea is to use Padé-theory techniques to continue analytically the sum of the perturbation theory expansion for the quasienergy calculated to a high order N: $E(E_0) = \sum_0^N a^{(2m)} E_0^{(2m)}$, to nonperturbative E_0, where the series no longer converges. The coefficients $a^{(2m)}$ can be obtained with good accuracy to high order. The method works for Rydberg states, as well for the ground state of H. QS was confirmed, and excellent agreement of the rates was found with Potvliege and Smith [61] and Potvliege and Shakeshaft [67]. The results for Re E were in very good agreement with those of Vos and Gavrila [39].

S-matrix theory, one of the major approaches of scattering theory, has also been applied to derive multiphoton ionization rates. In principle, its predictions should be equivalent to those of the Hamiltonian theories (Floquet theory, TDSE wavepacket calculations), but in practice the results have differed because of the approximations made. The Hamiltonian is split into a zero-order term plus a correction, and an expansion of the S-matrix with respect to the corrective term is carried out. To obtain tractable formulae, only lowest-order terms are retained. The result depends critically on the way the Hamiltonian is split, and on the 'in' or 'out' forms used for the matrix element. The approximate matrix element S_{fi} is eventually obtained as an infinite sum over n-photon contributions $S_{fi}^{(n)}$ of the form $S_{fi} = \sum_n \delta(W_f - W_i - n\omega) S_{fi}^{(n)}$, with analytical expressions for the $S_{fi}^{(n)}$. The stumbling block is that the eigenvalues in $\delta(W_f - W_i - n\omega)$ pertain to the Hamiltonian of the zeroth approximation and, for the choices made, they did not adequately represent the atom in a high-intensity field. This jeopardizes the result of setting $S_{fi}^{(n)}$ on the energy shell. (In principle, the energy conservation equation could be improved, by including higher-order terms in the S-matrix expansion, but this was not done.)

An early attempt along this line was that by Gersten and Mittleman [88, 89], sometimes inadvertently considered to be a precursor of QS as resulting from HFFT. This is not substantiated by a closer reading. Indeed, whereas HFFT operates under the high-frequency condition (5), which for H reads basically $\omega > 0.5$ au, these authors considered their theory to be low frequency, restricted by the condition $\omega < 0.5$ au. The energy conservation equations used, $W_f = W_i + n\omega$, were inadequate at high intensities (both at low and high frequencies), because they contained unperturbed energy levels (see [88, equation (3.7)]). As a consequence, the well established channel closure at low frequency and high intensity cannot occur. Moreover, the expressions for the rates derived differ from those of the HFFT, both for circular and linear polarizations (compare with our equations (11) and (12)).

S-matrix theory for strong fields was developed later more systematically by Reiss (see [90, 91], and also [15]). In the energy conservation equations used, the binding energies of the atom in the field were approximated by unperturbed binding energies plus the ponderomotive energy due to the field [90, equation (35)]. Consequently, the binding energies *increase indefinitely* with the field intensity, to the effect that all ionization channels close successively [91, figure 3], irrespective of frequency. At high frequencies this contradicts the numerical results of Hamiltonian theories. All Hamiltonian theories predict that the binding energy of an atom *decreases* with intensity (see, e.g., figure 1). For Floquet-type predictions, this follows from the work by Dörr *et al* [50, 55]. It follows also from the TDSE study of the energy of ejected electrons, as was shown convincingly by Su and Eberly [92]. Consequently, the *S*-matrix stabilization curves obtained in [91, figure 3] differ from those of HFFT (see our figure 2) and full Floquet theories (e.g., [50, figure 1]).

Other methods for determining quasienergies use TDSE. One of them is *spectral analysis*. The autocorrelation function $\langle\Psi(\boldsymbol{r},0)|\Psi(\boldsymbol{r},t)\rangle$ of a wavepacket $\Psi(\boldsymbol{r},t)$ evolving in a constant amplitude monochromatic field, with its initial condition $\Psi(\boldsymbol{r},0)$, is computed numerically. By Fourier transforming, the quasienergy spectrum of the states present in $\Psi(\boldsymbol{r},t)$ can be extracted. In the presence of closely lying quasienergies special precautions need to be taken (e.g. filter diagonalization). The potential of the method was demonstrated by Millack [76] in a 1D study of QS[14]. QS and the existence of oscillations in the large-α_0 behaviour of Γ [44] were confirmed.

Another such TDSE method, denoted as the '(t,t') *method*', was developed by Peshkin and Moiseyev [75]. It is based on treating the time as a dynamic variable in an extended Hilbert space of space-time functions. Thus, procedures from time-independent scattering theory ('half-collision' case) can be implemented. By applying further complex scaling techniques, it was shown that numerical results could be obtained for the quasienergies. As an illustration, the oscillatory behaviour of the ionization rate in the QS regime for 1D models [44] was regained. The method was also applied to calculate the decay rate Γ of the autoionizing doubly excited state $(2s)^2$ of He in a linearly polarized laser field [95]. It was found that a QS regime does indeed exist. Its onset was interpreted as being due to the suppression of electronic correlation, when the doubly excited state dichotomizes into the form for a double-well dressed potential (see end of section 2.1.2). For $\omega = 5$ eV (KrF laser), the beginning of the QS range (maximum of Γ) was calculated to occur at the accessible intensity of 2.3×10^{15} W cm^{-2}.

A *semiclassical approximation* was developed by Ivanov *et al* [96]. By writing the wavefunction as $\Psi(x,t) = \exp[\mathrm{i}S(x,t)]$ and assuming classical conditions (neglect of the classically unaccessible areas, where $E < V(x)$), $S(x,t)$ is real and satisfies the Hamilton–Jacobi equation. $S(x,t)$ is then decomposed as $S = S_1 + S_2 + \sigma$, where S_1 represents the known field-free motion in the atomic potential, S_2 the known free-electron motion in the laser field and σ the unknown interaction of the two motions. The assumption is made that the atomic motion is slow with respect that of the free electron in the field, and that the excursion amplitude corresponding to motion S_2 is small with respect to the size of the S_1 orbit. By then applying known classical procedures for dealing with this situation, σ was determined analytically. Returning to $\Psi(x,t)$, multiphoton transition probabilities could be derived. Specific cases of laser radiation interacting with high-lying Rydberg states were considered, and ionization rates could be calculated analytically; these manifest QS. One of these cases was shown to confirm the model of Rydberg state 'interference stabilization' developed over the years by Fedorov and collaborators (see [97–99], and also [15]).

[14] It was shown that the method can achieve comparable accuracy with Floquet methods [93] (see also [94]).

3. Dynamic stabilization

We have so far discussed QS as predicted (primarily) by Floquet solutions of TDSE. These, however, are special non-normalizable solutions satisfying peculiar boundary conditions. On the other hand, according to quantum mechanics, normalized wavepackets are the ones that carry the physical information. The natural question arises: is there a form of stabilization for one-electron atoms emerging from the wavepacket description of TDSE? If so, what is the connection with QS? Does stabilization also exist in classical dynamics? These, and related questions, will be addressed in the present section.

3.1. Wavepacket calculations

In typical experiments, a laser pulse of finite duration τ acts on an atom initially in some field-free energy eigenstate, leaving it in some continuum field-free state. The outcome is characterized by measured ionization yields. To simulate this situation theoretically, a wavepacket $\Psi(t)$ is propagated numerically in the laboratory frame (in the length or velocity gauges), starting from the specified initial condition. The ionization probability density per energy interval at the end of the pulse, $P_E(\tau)$, is given quantum mechanically by $P_E(\tau) = \sum_\gamma |\langle u_{E,\gamma}|\Psi(\tau)\rangle|^2$, where $u_{E,\gamma}$ is assumed to be the energy-normalized continuum solution, and γ a possible degeneracy label. The total ionization probability is

$$P_{ion}(\tau) \equiv \int P_E(\tau)\,\mathrm{d}E = 1 - \sum_n P_n(\tau), \tag{15}$$

where $P_n(\tau)$ is the excitation probability to the discrete state n. The sometimes displayed $P_{ion}(t)$ at times $0 \leqslant t \leqslant \tau$ during the pulse does not have physical significance, as only for $t \geqslant \tau$ does the Hamiltonian again become time independent.

For arbitrary polarization, the field of the laser pulse can be written as

$$\boldsymbol{F}(t) = F_0[f(t)\sin\omega t\,\boldsymbol{e}_1 + g(t)\cos\omega t\,\boldsymbol{e}_2], \tag{16}$$

where $\boldsymbol{F}(t)$ can be either the electric field $\boldsymbol{E}(t)$, or the vector potential $\boldsymbol{A}(t)$. For arbitrary polarization, the pulse has two different shape functions $f(t)$, $g(t)$, along the axes $\boldsymbol{e}_1$, $\boldsymbol{e}_2$, respectively; F_0 is the overall peak value. For linear polarization, the case most investigated, $g = 0$. The shape functions considered have had various kinds of turn-on and turn-off (more frequently linear, $\sin^2$; seldom Gaussian, sech), and, possibly, a flat top in between[15].

It was recognized early on (see, e.g., [100, 101]), and emphasized in recent mathematical studies (e.g. [102–104]), that the displacement $(\delta\boldsymbol{r})_\tau$ and the drift momentum $(\delta\boldsymbol{p})_\tau$, acquired by a *free* classical electron during the pulse

$$(\delta\boldsymbol{r})_\tau \equiv \boldsymbol{\alpha}(\tau) = \frac{1}{c}\int_0^\tau \boldsymbol{A}(t')\,\mathrm{d}t', \qquad (\delta\boldsymbol{p})_\tau \equiv \dot{\boldsymbol{\alpha}}(\tau) = -\int_0^\tau \boldsymbol{E}(t')\,\mathrm{d}t', \tag{17}$$

are relevant for the value of P_{ion} of an atomic electron driven by the same pulse. Indeed, if the field is strong, the effect of the nuclear force on the motion of the atomic electron is practically negligible, so that the electron behaves like a free particle during most of its oscillation. If these quantities vanish at the end of the pulse, or are small, the electron has more chance of being recaptured by the nucleus (survival of the neutral atom) than otherwise; see also further on, section 3.2, equation (26).

[15] Although the pulse was most of the time smoothly turned on, it was often discontinuously turned off. This renders the extraction of a final value for $P_{ion}(\tau)$ difficult, because then $P_{ion}(\tau)$ has large oscillations with respect to τ; in the realistic case with a smooth turn-off, these oscillations are damped, so that the value of P_{ion} emerges neatly; e.g., see [106, figure 17].

Theoretically, pulse envelopes can be chosen arbitrarily, so that $(\delta \boldsymbol{r})_\tau$ and $(\delta \boldsymbol{p})_\tau$ need not be vanishing, or small. Many calculations have been done under such circumstances. It has been recently realized, however, that there are experimental constraints imposed by the optical media generating the pulses. H G Muller has pointed out that physical pulses need to satisfy the conditions (see [17])[16]

$$\int_0^\tau \boldsymbol{A}(t')\,\mathrm{d}t' = 0, \qquad \int_0^\tau \boldsymbol{E}(t')\,\mathrm{d}t' = 0. \tag{18}$$

Combining equations (17) and (18) leads, for physical pulses, to

$$(\delta \boldsymbol{r})_\tau = 0, \qquad (\delta \boldsymbol{p})_\tau = 0. \tag{19}$$

Thus, the experimental conditions automatically impose the ideal situation for atomic survival (in NR dynamics).

Equations (15)–(19) were written for the case of pulses with finite duration τ (e.g. $\sin^2$). For pulses with infinite duration (e.g. Gaussian, sech), characterized by an FWHM (full width at half maximum) τ_p, the integrals need to be extended from $-\infty$ to $+\infty$.

3.1.1. Model studies. The wavepacket version of stabilization was discovered by Su, Eberly and Javanainen (1990) [2] for a 1D atomic model; this and later work of the group was summarized by Eberly *et al* [105] and Su [106]. Many calculations followed. They were done either in the laboratory frame or in the oscillating KH frame, by using short-range potentials or 'soft-core' Coulomb potentials. Short-range potentials sustain a finite number of levels, whereas Coulomb-tail potentials (behaving like $1/|x|$ at infinity) sustain an infinite series of Rydberg states. 'Soft-core' Coulomb potentials have the $1/|x|$ singularity at the origin softened (replaced by a 'soft core') such that $V(0)$ is finite, to make the problem tractable in one dimension. It turns out that the stabilization results are rather insensitive to the potential model chosen within each of the two categories. Note that the pulses used in earlier papers did not always satisfy the necessary conditions (equation (18)), which were not known at the time.

These TDSE studies have shown that for one-electron atoms subject to pulses of fixed shape as in equation (16), P_{ion} does not rise to unity as the peak amplitude F_0 increases, as might have been expected. Instead, beyond some critical field value, P_{ion} either *decreases* (possibly in an oscillatory manner), or presents a *plateau behaviour*, levelling off at some value $P_{ion} < 1$. This phenomenon has been termed 'dynamic stabilization (DS)'[17]. All calculations, with one exception, have confirmed the existence of DS (see section 3.3).

We emphasize that, whereas QS characterizes an intrinsic property of the atom (specifically, of its modes of ionization), DS depends critically on the laser pulse applied, i.e. on the manner in which the atom is handled experimentally. As with QS, we are dealing here with a counter-intuitive effect, when more driving force applied to the atom generates less, or the same response.

Further 1D calculations of DS for a soft-core Coulomb potential were done by Wiedemann *et al* [107], Su *et al* [108] and Florescu *et al* [109]. For short-range potentials, work has been done on the screened soft-core Coulomb potential by Patel *et al* [110], and on the δ potential, $V(x) = -B\delta(x)$. The δ potential has been a source of controversy: some authors have found DS for it (Sonnenmoser [101], Su *et al* [111], Geltman [112], Dörr and Potvliege [113]),

[16] The Muller argument runs as follows. Experimentally, the low-frequency Fourier components $\boldsymbol{E}_0(\omega)$ of the electric field $\boldsymbol{E}(t)$ are suppressed by optical materials: $\boldsymbol{E}_0(\omega) \to 0$, as $\omega \to 0$. Using the integral expression of $\boldsymbol{E}_0(\omega)$ in terms of $\boldsymbol{E}(t)$, this is expressed in terms of the second condition of equation (18). Further, as $\boldsymbol{E}_0(\omega) = (\omega/c)\boldsymbol{A}_0(\omega)$, if $\boldsymbol{E}_0(\omega) \to 0$ sufficiently rapidly, also $\boldsymbol{A}_0(\omega) \to 0$, which is expressed by the first condition of equation (18).

[17] In contrast to [17], we are including here in the definition of DS the possibility that P_{ion} has a plateau behaviour at $P_{ion} < 1$, in order to encompass the recent findings discussed in section 3.1.2.

whereas others have not (Geltman, in his earlier papers [114], Mercouris and Nicolaides [115]). The issue will be discussed in section 3.3.

We shall now present 1D results for DS from two recent calculations. The first one, by Su *et al* [108], is the evaluation of P_{ion} for the soft-core Coulomb potential $V_s(x) = -(1+x^2)^{-1/2}$ (binding energy 0.67 au). A laser pulse of the form of equation (16) for the electric field $E(t)$ was applied, the envelope $E_0(t)$ having a $\sin^2$ turn-on/off of length $\tau_0 = 5$ cycles, and a flat top of length $T = 40$ cycles in between; the frequency was $\omega = 0.8$ (a high-frequency situation). The peak field E_0 was varied from zero to large values. For this pulse, conditions (18) are only partially satisfied (resulting in $(\delta p)_\tau = 0$, $(\delta x)_\tau \neq 0$). The calculation displays the following ionization regimes (see [108, figure 1]). First comes the *LOPT regime*, at small intensities, in which P_{ion} is roughly proportional with I, as expected. This is followed by the *'death valley' regime*[18], occurring at intensities of about 1 au, where P_{ion} is close to unity. An atom subject to a pulse with peak intensity in this range has little chance of surviving in a neutral state. Thereafter, we have the *DS regime*, in which P_{ion} decreases slowly with I, albeit in an oscillatory manner (an interpretation of the origin of the oscillations was given in [108], see also [113]). Note that although conditions (19)) are not satisfied, the model does display DS. At still higher intensities ($I \gtrsim 10^2$ au), this calculation shows the existence of a 'destabilization regime', in which P_{ion} increases again. This occurrence will be discussed in section 3.2.

Figure 3 shows the recalculation by Florescu *et al* [109] of the result by Su *et al* [108]. Along with the case $T = 40$ cycles considered in [108], also included are the cases $T = 0$ (purely $\sin^2$ envelope) and $T = 10$, all at $\tau_0 = 5$ cycles[19]. The four regimes of P_{ion} are apparent. Ionization is stronger at larger T, as there is more time for ionization during the flat top of the pulse. Moreover, for all values of T there is a high amount of survival probability at the minimum of P_{ion} (separating the stabilization and destabilization regimes), where $P_{ion} \approx 0.2$.

The second calculation we consider, due to Patel *et al* [110], is a systematic study of P_{ion} for the potential $V(x) = -(2+x^2)^{-1/2}\exp(-x^2/\beta^2)$, for $3 \leqslant \beta \leqslant 75$, with a ground-state binding energy of about -0.5 au. Although this is a short-range potential that supports only a finite number of bound states, as β becomes large their number increases, and they approach the levels of the soft-core Coulomb potential: $-(2+x^2)^{-1/2}$. The laser pulses were taken as in equation (16), with $f(t) = \sin^2(\pi t/\tau)$, in one case for $A(t)$, and in the other for $E(t)$. The frequency was $\omega = 1$ (a high-frequency case), and E_0 and τ were varied over the ranges $0 \leqslant E_0 \leqslant 50$ au and $0 \leqslant \tau \leqslant 50$ cycles. The quantities in equation (17) were also calculated. For the $A(t)$ pulse, $(\delta p)_\tau$ is always vanishing, but $(\delta x)_\tau$ vanishes only if τ is an integer number of cycles, i.e. condition (19) is only partly satisfied. The results were presented in the form of 3D graphs for $P_{ion}(E_0, \tau)$ (see [110, figures 2 and 3]); the plane wave connection $E_0 = \omega A_0/c$ was adopted to translate the peak value A_0 of the $A(t)$ pulse into an E_0 amplitude. We reproduce in figure 4 the results for the $A(t)$ pulse. Sections through the surface $P_{ion}(E_0, \tau)$ at a larger τ yield curves similar to those in figure 3, confirming the existence of the DS regime. (The difference in aspect of figures 3 and 4 stems mainly from the different scales used on the abscissa.) Very short pulses yield a different pattern for P_{ion}: following a steep rise with E_0, P_{ion} stays nearly constant.

By varying the range of the potential β, one could investigate the effect of the number of bound states on DS. It was shown that the more bound states the potential has, the smaller $P_{ion}(E_0, \tau)$ becomes for the same pulse, which enhances DS. Also, the effect on DS of the nonobedience of conditions (18) was considered. This is attenuated for long-range potentials, because, although now $(\delta \boldsymbol{r})_\tau$, $(\delta \boldsymbol{p})_\tau$ are nonzero, the electron can still be trapped at the end

[18] We use this terminology because the *death valley* of wavepacket calculations corresponds to that of Floquet calculations (see section 2.1.3).

[19] At $T = 40$ the agreement between calculations [109] and [108] is at the graphical level.

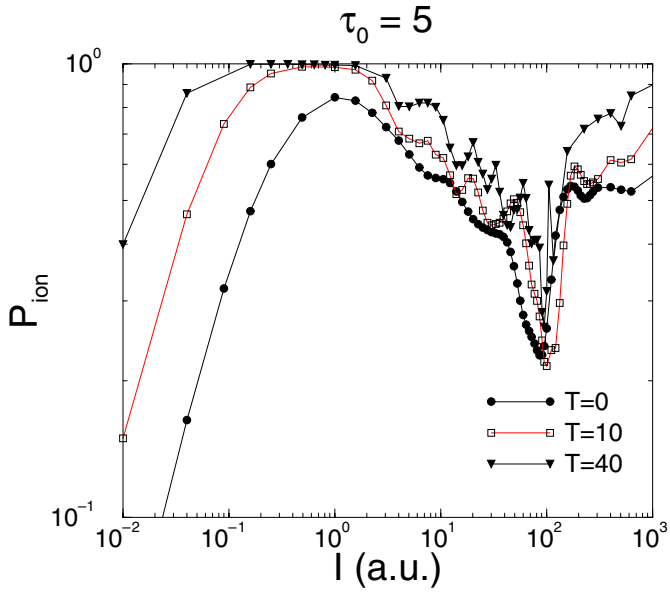

Figure 3. Total ionization probability for a 1D model with soft Coulomb potential (binding energy 0.67 au). Laser pulse for $E(t)$, of frequency $\omega = 0.8$ au, with $\sin^2$ turn-on/off of five cycles, and a flat top of T cycles in between, as calculated by Florescu *et al* [109]. Calculation at $T = 0$ was originally done by Su *et al* [108].

(This figure is in colour only in the electronic version)

of the pulse in highly excited states (with large spatial extension), whereas this cannot happen for short-range potentials with few, tightly bound states.

2D and 3D models have also been considered. Recent calculations by Patel *et al* [116, 117], in two dimensions, have concentrated on a soft Coulomb potential of the form $V(x, y) = -(a^2 + x^2 + y^2)^{-1/2}$, and have studied the evolution of $|\Psi(x, y, t)|^2$ for various degrees of ellipticity. A comon field envelope was taken in equation (16), $f(t) = g(t)$, for the short trapezoidal pulses of circular polarization used; see, however, the remark at the end of section 3.1.3. $|\Psi(x, y, t)|^2$ displayed rotating ring structures, indicative of the presence in $\Psi(x, y, t)$ of superpositions of dressed HFFT states for circular polarization, excited during a nonadiabatic turn-on. At frequency $\omega = 1$, DS was found to exist for arbitrary polarization, 'death valley' being deeper for circular than for linear polarization. A similar study, for the same potential and circular polarization, was carried out by Chism *et al* [118] at $\omega = 1.2$. A rotating ring structure was again found for $|\Psi(x, y, t)|^2$, and compared to [117, figure 2]. A calculation of the lifetimes [118, figure 1], however, resulted in excessively high values at larger fields, out of line with 3D calculations for H [27, figure 18], and [142].

3D DS from excited states of H (linear polarization) was studied by Popov *et al* (see [119], and references therein), using a soft-core Coulomb potential. The states considered were $n = 3$ and all possible l, m values. Photon energy was $\omega = 5$ eV, larger than the binding energy of the states, but smaller than that for 1s. The states which were lowest in the magnetic manifolds $m = 1, 2$ (e.g. 3p, $m = 1$; 3d, $m = 2$) satisfied unambiguously the high-frequency condition $\omega > W_{exc}^{(m)}$, and displayed ionization curves P_{ion} with one maximum, followed by DS, as for the ground state [119, figure 1]. For the states lying higher in the magnetic manifold $m = 0$, more complicated shapes appear.

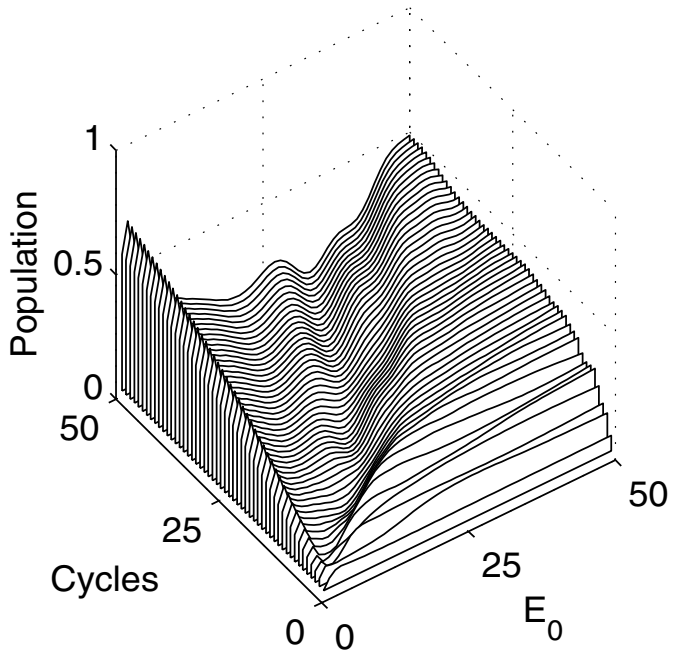

Figure 4. Ionization probability for a 1D model (see text), following a pulse $A(t) = A_0 \sin^2(\pi t/\tau) \sin \omega t$, with $0 < t < \tau$, $\omega = 1$ au, variable duration τ (in cycles) and peak amplitude $E_0 \equiv \omega$, A_0/c (from Patel *et al* [110, figure 2]).

A 3D short-range potential model with a soft core and one level only was studied by Tikhonova *et al* ([120] and references therein). Three frequencies were considered: one decidedly HF, the others only marginally so. The first one presented the usual HF features, including DS. The other two appeared to display mixed low- and high-frequency features, e.g. channel closure at low intensity, followed by LIS appearance, and HF behaviour at large intensity.

Two-electron atoms have also been explored with 1D models, including correlation. The potentials considered were of the soft-Coulomb form, $V(x) \sim (a^2+x^2)^{-1/2}$, for both electron–nucleus, and electron–electron interactions. The two ionization potentials W_1 and W_2, for one- and two-electron ionization respectively, are now natural terms of comparison for ω. The search for DS in the one-electron ionization probability was carried out by Grobe and Eberly [121] (H^-), and Bauer and Ceccherini [122] (He). Their findings are divergent, possibly due to the different ionization regimes involved. Thus, for $W_1 < \omega < W_2$, DS was found in [121] but not in [122], and for $\omega > W_1, W_2$, DS was found in [122], but not in [121]. Further study is needed. The analysis of $|\Psi(x_1, x_2, t)|^2$ in [122] yielded a predominantly dichotomous structure during the flat top of a not too rapidly turned on pulse, as would be expected from the two-electron HFFT (see [63, 64], and section 2.1.2).

3.1.2. Realistic 3D calculations. Fully-fledged 3D calculations for DS in the ground state of H were carried out first by Kulander *et al* [123] (see also [124]), Tang and Basile [125] and Horbatsch [126]. The work by Kulander and collaborators was done in the length gauge, while that by Tang and Basile was done in the velocity gauge, identified as the most convenient for the laboratory frame; the work by Horbatsch was done in the oscillating frame. A main thrust in [123] and [126] was to establish the connection between DS and QS, by extracting rates

from TDSE wavepackets Ψ. By considering slowly turned on pulses with a flat top, from the (quasi) exponential decay during the flat top of either the norm of Ψ in a sphere of radius R, or of the projection of Ψ on the unperturbed ground state, rates Γ were extracted. These were then compared with Floquet results. Although the accuracy was limited at the time, QS was clearly confirmed. Subsequently, Latinne *et al* [127] carried out a 3D calculation in order to test the validity of the dipole approximation (see section 4.2.2). In the process, dipole-approximation DS was confirmed for a quasiadiabatic pulse regime and H in the ground state [127, figure 2].

Tang and Basile [125] (see also Lambropoulos and Tang [128]) studied short pulses and the effect of the pulse duration on DS. They also compared the predictions of their 3D computation with results obtained from a typical 1D soft-core Coulomb model, in order to assess the merit of such models. A Gaussian envelope was used for $\boldsymbol{A}(t)$; equations (18) and (19) were satisfied to good accuracy. P_{ion} was evaluated rather accurately for $\omega = 1$, at a number of values of τ (4π, 10π, 20π au), and several peak intensities I (0.2, 1, 5, 25 and 100 au)[20]. They found that the 1D model substantially exaggerated the survival probability and DS in comparison to the 3D case. Moreover, from their numerical 3D results they concluded that an experimental demonstration of DS for the ground state of H was out of reach for the 'foreseeable future'. The conclusion reflected the experimental limitations at the time, when none of the necessary laser prerequisites were available: high frequencies, high intensities and very short pulses.

This realization has channelled attention to DS of excited states of H (see also sections 2.1.1 and 4). Pont *et al* [129, 59] (see also [130]) have considered linear polarization at $\omega = 0.2$ au, an energy that is high with respect to the binding energies of the $n \geqslant 3$ states considered, and within experimental reach. They ascertained that DS did exist for these cases. The fact that DS can occur for photon energies *below* the ionization potential of the field-free state was confirmed for H by Huens and Piraux [131] (a situation already encountered in 1D calculations, e.g. [2]). The state chosen was 2s, and Gaussian pulses of linear polarization and various durations were applied. By considering the population distribution at the end of the pulse, it was also shown that, for short pulses or high intensities, much of the population is projected into excited states, which sheds light on the physical origin of DS (see section 3.2). The paper by Gajda *et al* [132] is one of the few that have studied DS numerically for circular polarization. The vector potential $\boldsymbol{A}(t)$ was taken similarly to equation (16), with $g(t) = f(t)$ (see, however, the remark at the end of this section). The excited states 2p, $m = 0, \pm 1$ and the relatively high frequency $\omega = 0.25$ au were chosen. For the $m = 0, 1$ substates, DS was conspicuous, whereas for $m = -1$ it was much weaker at the intensities considered. Piraux and Potvliege [133] have studied the 5g, $m = 4$ state, appearing in the experiments of Muller and collaborators; we discuss the results in section 4.

A recent paper by Bauer *et al* [134] has readdressed the issue of ground-state stabilization of H, after a long lapse of time; one case of DS was studied ($\sin^2$ pulses at $\omega = 50$ eV, 30 cycles duration), and two cases of QS (at $\omega = 17$ and 50 eV), both for linear polarization.

A *comprehensive computation* of DS for the ground state and linear polarization was finally carried out by Dondera *et al* [135] (pulses of finite duration), [136] (pulses of infinite duration), in which P_{ion} was mapped out over extended ranges of high frequencies ($0.51 < \omega < 8$ au), peak field amplitudes ($0 < E_0 < 80$ au, depending on ω), for various pulse envelopes (sech, Gaussian and $\cos^2$) and FWHM pulse durations τ_p ($1 < \tau_p < 100$ cycles, depending on ω). The computation was motivated by the advent of high-frequency light sources: VUV-FELs, that are now in test operation (HASYLAB at DESY, [137, 138]) or under construction (BNL), and attosecond pulses produced by high-harmonic generation [139, 140].

[20] These calculations were repeated in a few cases by Dondera *et al* [136], and the agreement was within a few tenths of one per cent.

The TDSE was integrated in the velocity gauge using a highly efficient numerical program, exhaustively optimized [141], and retested at high frequencies with excellent results. The accuracy on P_{ion} was estimated at better than 1%. The pulses considered were linearly polarized, of the form equation (16) for $\boldsymbol{A}(t)$. The following choices of shape functions were made:

$$\begin{aligned} f_{sh}(t) &= \operatorname{sech}(1.763t/\tau_p), \\ f_g(t) &= \exp[-(1.177t/\tau_p)^2], \\ f_c(t) &= \cos^2(1.144t/\tau_p), \qquad |t| < \pi\tau_p/2.288, \end{aligned} \tag{20}$$

where τ_p represents FWHM[21] for $\boldsymbol{A}^2$. These functions are very much alike in their central parts ($-\tau_p/2 < t < +\tau_p/2$), but differ substantially in the shape of their wings. Their choice has an exploratory character, as it is not clear what the pulses produced by the high-frequency light sources will look like. All these pulses satisfy the requirements of equations (18) and (19), for *any* τ_p.

Figures 5–8 show results for P_{ion} at $\omega = 1$, 2, 4 and 8. A nominal peak electric field E_0 was introduced for reference, via the plane wave connection: $E_0 = (\omega A_0/c)$. (It can actually be shown that E_0 coincides with the peak value of the electric field of the pulse.) The values of E_0 considered extend up to about the limit at which nonrelativistic (NR) calculations are expected to be valid (see section 4.2). For *longer pulses*, the figures show a dependence of P_{ion} on E_0 similar to that emerging from 1D calculations (see figure 4): an incipient growth with E_0, followed by a maximum and then by a monotonic decrease (for sech pulses this is more like a plateau). The latter regime is that of DS, quite prominent in all cases. It was confirmed that 1D model calculations, done under similar pulse conditions, yield misleadingly small P_{ion}. Moreover, in contrast to the 1D case (see figures 3 and 4), P_{ion} has no oscillations in the DS regime. The dependence of P_{ion} on the pulse shape is quite marked. Since these pulses practically coincide in their central parts, the difference stems from the shape of their wings. The manifestation of DS is different for the $\cos^2$ pulses (finite extension) and Gaussian (infinite extension, but rapidly decreasing wings), on the one hand, and for the sech pulses (infinite extension, but more slowly decreasing wings), on the other. In the first case, P_{ion} is a decreasing function of E_0; in the second, the function is flat (with $P_{ion} < 1$). The dependence of P_{ion} on ω is quite strong, leading to more prominent DS and atomic survival as ω increases, but on the other hand requiring larger peak values E_0 for DS to set in. The longest τ_p leading to DS at a detectable value of P_{ion} (i.e. not too close to unity) is in the femtosecond range, and increases slowly with ω. *Short pulses* ($\tau_p < 1$) yield a different picture. For the extreme case of $\tau_p = 0.25$, P_{ion} becomes practically constant at large E_0 (more slowly at larger ω). For somewhat longer pulses (e.g. $\tau_p = 1$), this situation has not fully developed in the E_0 range shown, and P_{ion} is still in its growing stage.

The conclusion of the work by Dondera *et al* [135, 136] was that there is prominent DS in peak-field ranges where NR calculations should be valid, DS manifests a strong dependence on the shape of the pulse envelope and the evolution of the atom is remarkably adiabatic up to large fields and down to short pulses (see figure 9). The results indicate that DS should be observable with the new light sources (VUV-FELs or attosecond pulses generated by high-harmonic generation), albeit in a state-of-the-art experiment.

Meanwhile, using a similar numerical program, Boca *et al* [142] have investigated DS for the ground state of H, with circularly polarized radiation. The vector potential $\boldsymbol{A}(t)$ was taken as in equation (16), with $g(t) = f(t - 2\pi/\omega)$. This is required by the fact that the pulse component on one of the axes is retarded by a quarter wavelength with respect to the other axis (e.g., consider the case of quarter-wave plates). $f(t)$ was taken as in equation (20), and also

[21] For the $\cos^2$ pulse, the connection between the actual duration of the pulse τ and τ_p is $\tau = 2.75\tau_p$.

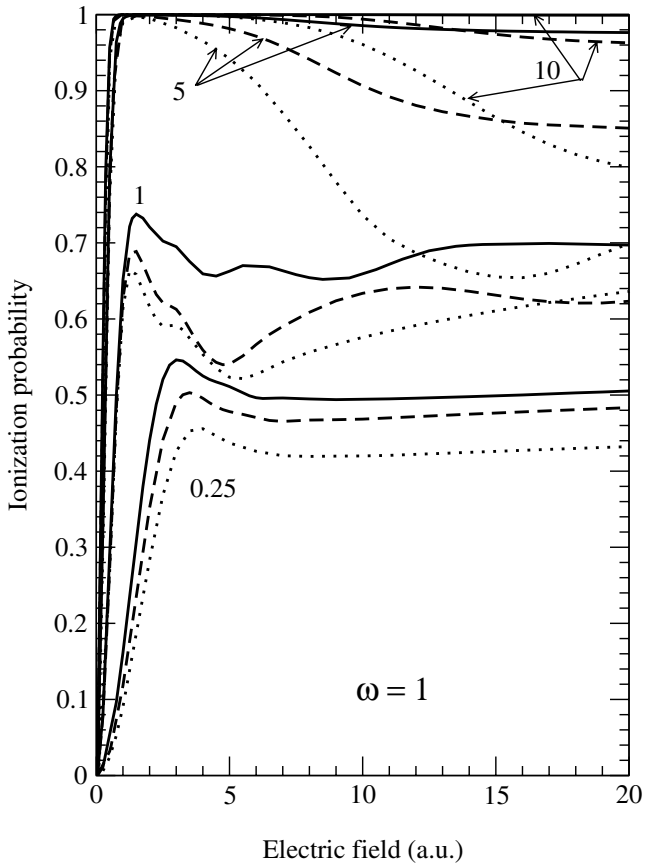

Figure 5. Ionization probability of ground-state H exposed to pulses with $\omega = 1$ au and one of the triplet of envelopes in equation (20), at various FWHM pulse durations τ_p, as a function of the peak field E_0 (in au). Sech pulses, solid curves; Gaussian pulses, dashed curves; $\cos^2$ pulses, dotted curves. The value of τ_p, in cycles, is specified for each triplet of envelopes (the corresponding values P_{ion} coalesce at small E_0) (from Dondera *et al* [136]).

of Lorentzian form: $f(t) = [1 + (1.29\,t/\tau_p^2)]^{-1}$. The results are qualitatively similar to those obtained for linear polarization. The same marked dependence of DS on the pulse envelope has emerged. In particular, for the Lorentzian envelope, no DS was found at all: P_{ion} continued to increase in the intensity ranges covered, a fact signalled by Piraux and Potvliege [133]. Our choice of $g(t)$, as opposed to taking $g(t) = f(t)$, has substantial effect for few-cycle pulses; for longer pulses ($\tau_p > 5$), the effect fades away.

3.2. Physical interpretation of DS. Connection with QS

The existence of DS ascertained, we shall now enquire into the physical origin of the phenomenon. We shall also answer the question of its connection with QS. The issues are subtle, and their elucidation was slow to come.

It has been realized that a useful approach for describing high-frequency phenomena, including DS, is to analyse wavepacket solutions $\Psi(\boldsymbol{r}, t)$ of equation (4) in terms of superpositions of dressed eigenstates $v_\nu(\boldsymbol{r}\,; \alpha_0)$ of the HFFT structure equation (equation (6)).

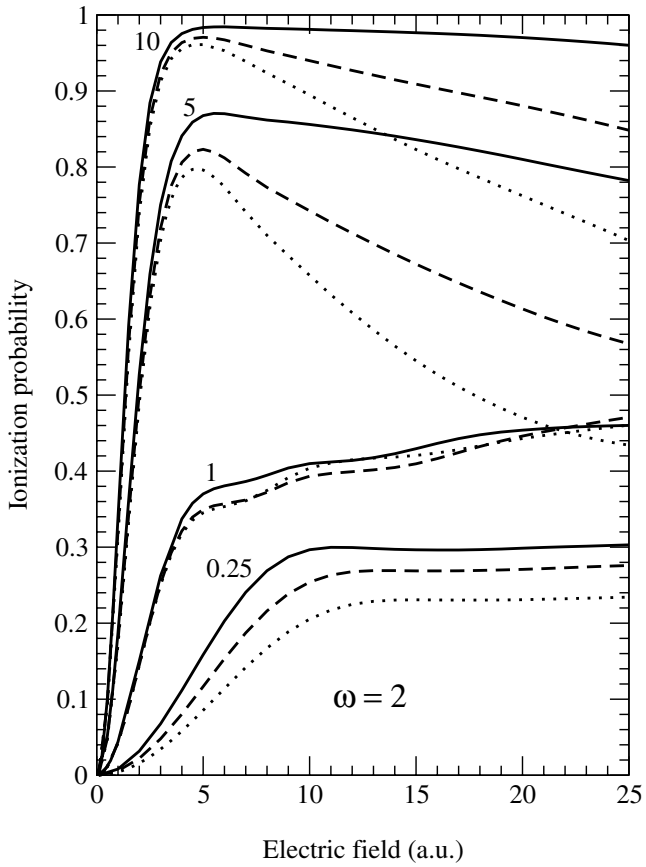

Figure 6. The same as for figure 5, except that $\omega = 2$.

It was shown in section 2.1.1 that in a field of constant amplitude these are approximate quasistationary states. As they form a complete set (at any α_0), the following expansion formula holds:

$$\Psi(\boldsymbol{r}, t) \propto \mathsf{S}_\nu d_\nu(t) \mathrm{e}^{-\mathrm{i}W_\nu t} v_\nu(\boldsymbol{r}, \alpha_0). \tag{21}$$

S_ν stands for summation over the discrete, and integration over the continuous spectrum. The coefficients $d_\nu(t)$ are time-dependent, even for a field of constant amplitude; they are constants only in the high-frequency limit.

Let us now consider the case of a laser pulse with time-dependent envelope, described by a certain $\boldsymbol{\alpha}(t)$, equation (2). In the exact space-translated Schrödinger equation, equation (4), the time dependence of the oscillating potential comes on the one hand from the rapid oscillations of the field, and on the other from the variation of the envelope. If the latter variation is slow during a period $2\pi/\omega$, one can average over the field oscillations (as was done in the stationary HFFT), which leads to

$$\left[\frac{1}{2}\boldsymbol{P}^2 + V_0(\alpha_0(t), \boldsymbol{r})\right]\Psi = \mathrm{i}\frac{\partial \Psi}{\partial t}. \tag{22}$$

By now expanding $\Psi(\boldsymbol{r}, t)$ in the instantaneous eigenfunctions $v_\nu(\boldsymbol{r}, \alpha_0(t))$ of the Hamiltonian in equation (22), one gets an extension of equation (21). The time dependence of the $d_\nu(t)$

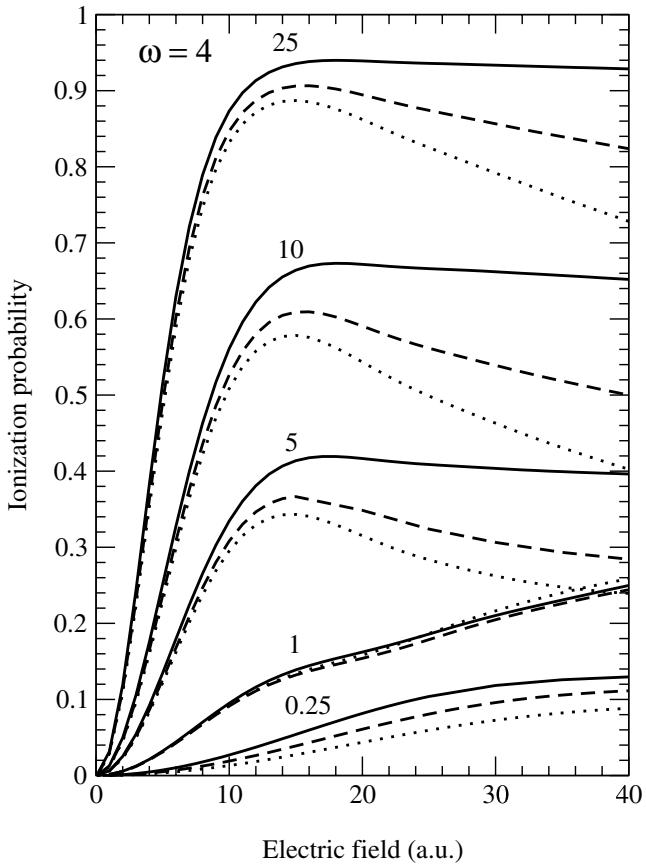

Figure 7. The same as for figure 5, except that $\omega = 4$.

can be determined by inserting $\Psi(\boldsymbol{r}, t)$ into equation (22). Patel *et al* [110] and Barash *et al* [143], have shown this high-frequency approximation to work rather well in practice.

Although the quantities $|d_v(t)|^2$ do not have, strictly speaking, an observable meaning during the pulse, they are useful to illustrate the population migration over the approximately stationary states v_v, and eventually into the field-free states. This has been illustrated in various ways, for example by considering the evolution of the probability density $P(\boldsymbol{r}, t) = |\Psi(\boldsymbol{r}, t)|^2$, or of the projection of $\Psi(\boldsymbol{r}, t)$ on bound states, $|d_v(t)|^2 = |\langle v_v|\Psi\rangle|^2$. If the pulse is not turned on too abruptly, and the initial state is the ground state, only *one or a few* lower discrete states $v_v(\boldsymbol{r}, \alpha_0)$ will be excited. This has a characteristic signature on the form of $P(\boldsymbol{r}, t)$ and $|d_v(t)|^2$. It should be kept in mind, however, that, all along, there is a slow but steady build-up of population in the continuum at the energies at which multiphoton ionization occurs.

Eberly and collaborators [2, 105, 106, 144], have followed the evolution of $P(x, t)$ for the 1D model with soft-core Coulomb potential $V_s(x)$, and shown that at large peak intensities $P(x, t)$ contains wavepacket portions flying towards $x = \pm\infty$, representing ionization, but that the dominant part of the wavepacket stays oscillating near the origin, at distances of order α_0. This occurrence has been termed *localization*, and is associated with large populations $|d_v(t)|^2$ in low-lying states (see, e.g., [106, section 4]). Were only the ground state present in the wavepacket equation (21), $P(x, t)$ would have an oscillatory 'dichotomous' form, of

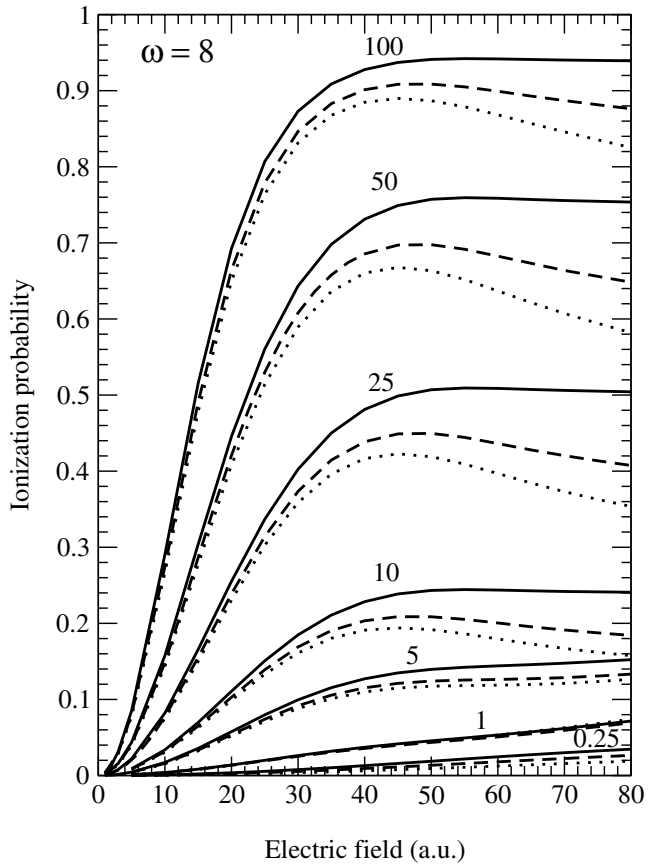

Figure 8. The same as for figure 5, except that $\omega = 8$.

the type discussed in section 2.1.1. In reality, because the pulses considered were rather short and ω not sufficiently high, the localized oscillating shapes found had a more complicated 'polychotomous' structure, indicating that several dressed states had been excited. This was confirmed in three dimensions by the detailed computations by Kulander *et al* [123, 124], who followed $P(\boldsymbol{r}, t)$ over many cycles; a movie of its motion was made (a primer, at the time).

The presence of only a few states in expansion equation (21) can also be inferred by looking at the oscillations undergone by the populations $|d_v(t)|^2$ in the lower v_v states. These populations exhibit, on top of the fast oscillations of frequency ω imposed by the laser, slow oscillations having the transition frequencies $|W_i - W_j|$ of the dressed states involved. The analysis was done for various initial conditions, by Law *et al* (qualitative) [145], Burnett *et al* (qualitative) [7], Vivirito and Knight (two-state model) [146] and Wells *et al* (virtually exact HFFT description) [35].

The study of ionizing wavepackets in terms of dressed states, equation (21), has been instrumental for the physical interpretation of DS and the identification of the relevant parameters (see the reviews by Eberly *et al* [105] and Burnett *et al* [7], also [147]). However, in order to establish a closer connection with Floquet theory, we shall adopt here for the interpretation of DS an expansion in terms of Floquet states. We recall that Floquet states

represent intrinsic modes of ionization of an atom, and are *exact* quasistationary solutions, for constant amplitude fields (see section 2.1.1).

The expansion formula we use is

$$\Psi(\boldsymbol{r}, t) \propto \mathsf{S}_\nu C_\nu(F_0)\psi^{(\nu)}(\boldsymbol{r}, t; F_0), \tag{23}$$

where $\psi^{(\nu)}(\boldsymbol{r}, t; F_0)$ are the Floquet states, equation (5), for the laboratory or the oscillating frame, and F_0 the field amplitude; ω is fixed and assumed high. (Depending on the calculation, F_0 can stand for E_0 or A_0.) The summation S_ν extends over discrete quasienergy states, but also includes an integration over continuum states along an adequate contour in the complex energy plane[22]. In a field of constant amplitude F_0, $C_\nu(F_0)$ are obviously constant; in a variable-amplitude field, they are time dependent, and $\psi^{(\nu)}(\boldsymbol{r}, t; F_0)$ acquires an extra time dependence due to $F_0(t)$. Because we are interested here in high ω (larger than the tightest binding energy in the field), the discrete states entering equation (23) cannot be connected resonantly by photon transitions; this has far-reaching consequences for the possible evolution of the system. Conceptually, equation (23) is a good tool for understanding the dynamics in strong fields in general, and in particular DS and its relation to QS. Equation (21) represents basically the high-frequency limit of equation (23) (see section 2.1.2).

The simplest case in which a system can be described in terms of equation (23) is that when the expansion contains approximately only one term, corresponding to an initial unperturbed state[23] $\psi^{(0)}$. This is the traditional *single-state Floquet theory*, presented in section 2. In this case, during the pulse we have $C_0 \approx 1$, $C_{\nu\neq 0} \approx 0$, in equation (23), and the energy of the system will follow in time the real part of the quasienergy Re E_0, from its field-free value to its peak-field value, and then back. Ionization occurs only from the state $\nu = 0$, with the instantaneous rate $\Gamma[F_0(t)]$. An analysis shows that, in order for this to be possible, several conditions should be met, e.g. see [13, section II]: Γ should be sufficiently small during the pulse, no multiphoton resonances with excited states should occur and the pulse should be 'adiabatically' turned on and off. At high frequencies the first condition can be easily met and the second is automatically fulfilled, so that the one to care about is the third. Adiabaticity means that the envelope of the pulse $F_0(t)$ varies sufficiently slowly, allowing the electronic motion to adjust continuously to the instantaneous value of the field intensity. The appropriate timescale depends on whether we are dealing with low-lying states, or Rydberg states.

Under the adiabatic condition, simple reasoning yields the following formula for the ionization probability P_{ion} at the end of the pulse:

$$P_{ion}^{(ad)} = 1 - \exp\left[-\int_{-\infty}^{+\infty} \Gamma[F_0(t)]\,\mathrm{d}t\right]. \tag{24}$$

Whereas the formula is intuitive, rigorous mathematical analysis shows its limitations (e.g. Mittleman and Tip [148]). Conversely, if the dynamically computed P_{ion} coincides with $P_{ion}^{(ad)}$, this indicates the presence of only one state in the expansion equation (23).

The remarkable extent to which the dynamic P_{ion} is approximated in practice by $P_{ion}^{(ad)}$ has been signalled by Zakrzewski and Delande [77]. They compared the results for $P_{ion}^{(ad)}$ from their Floquet calculations for the initial states 2p, $m = 0, \pm 1$, of H with the dynamically calculated P_{ion}, for the same pulse conditions ($\sin^2$ pulse of 20 cycles, at $\omega = 0.25$ au) by Gajda *et al*

[22] Expansion equation (23) expresses the *mathematical completeness* of the Floquet system of states. This is a delicate property, which was rigorously proven for the case when the quasienergies are real, i.e. the Floquet states have scattering boundary conditions, but has still to be worked out for the case of Gamow–Siegert boundary conditions. For comments and references, see Wells *et al* [35].

[23] The unbounded asymptotic behaviour of $\psi^{(0)}$ requires the presence of a weak admixture of continuum states in the expansion equation (23), whose destructive interference with $\psi^{(0)}$ can ensure the normalization of the wavepacket $\Psi(\boldsymbol{r}, t)$.

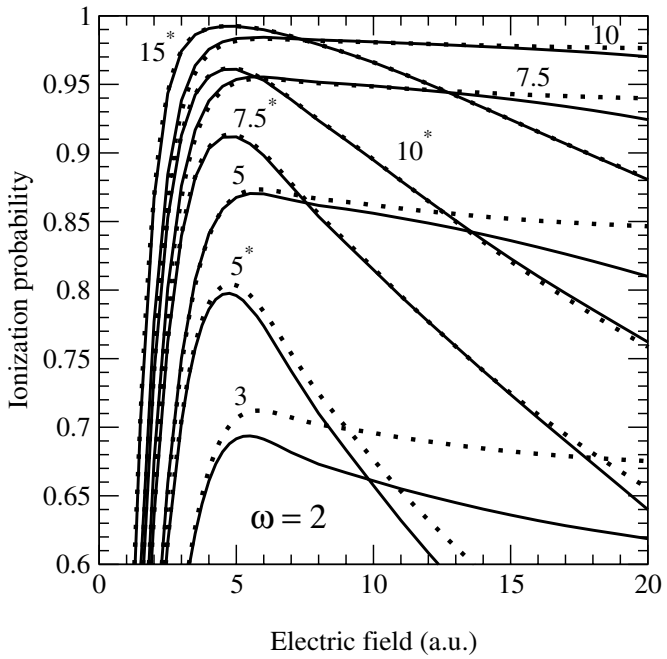

Figure 9. Comparison at $\omega = 2$ of the E_0 dependence of the computed ionization probability of ground-state H (full curves) and the adiabatic approximation equation (24) (dotted curves). The values of τ_p, in cycles, are given for pairs of such curves. Sech and $\cos^2$ pulses are presented; $\cos^2$ pulses are distinguished by an asterisk on their τ_p value (from Dondera *et al* [136]).

[132], and found surprising agreement. The agreement covered the range of peak fields E_0, in which $\Gamma(E_0(t))$ manifested QS, and P_{ion} manifested DS. The result was confirmed by other calculations for the H atom, done by Piraux and Potvliege [133, e.g., see table 1] (Rydberg state) and Dondera *et al* [135, 136] (ground state), and by the 1D calculations of Dörr and Potvliege [113, figure 1]. We show in figure 9 a comparison at $\omega = 2$ of P_{ion} and $P_{ion}^{(ad)}$ for the ground state of H, according to Dondera *et al* [136]. Two types of pulse are shown, sech and $\cos^2$, as defined by equation (20). Obviously, the larger τ_p, the better the two results agree. It is apparent that, for the pulse shapes considered, the evolution of the atom is, indeed, remarkably adiabatic up to quite high values of E_0 (e.g. $E_0 < 10$), even for short pulses ($\tau_p \widetilde{=} 5$), and that the agreement extends well into the DS regime.

As discussed in section 2, for ground states, $\Gamma^{(0)}(F_0)$ starts by increasing with F_0, passes a maximum (corresponding to *death valley* of the lifetime), and thereafter decreases, undergoing QS. This behaviour of the rate has to be convoluted with the pulse shape in order to get $P_{ion}^{(ad)}$ of equation (24). The result may display DS or not, depending critically on the pulse shape. For narrow-wing pulses ($\cos^2$, Gaussian) $P_{ion}^{(ad)}$ is decreasing (on average) with F_0; for broader-wing pulses (sech) it has a plateau (see figures 3 and 4 for the 1D case, and figures 5–9 for the 3D case). Hence, for adiabatic pulses of these types DS is a consequence of the underlying QS. On the other hand, very broad-wing pulses (e.g. Lorentzian) lead to monotonically growing $P_{ion}^{(ad)}$, i.e. no DS (Boca *et al* [142]). A similar situation was signalled for Rydberg states by Piraux and Potvliege [133]. Conversely, at given pulse, $P_{ion}^{(ad)}$ is quite sensitive to the form of $\Gamma(F_0)$ of the state considered, and can manifest DS or not; this is illustrated by figures 2–4 of [77].

Until recently, the criterion of adiabaticity was not much of a limitation, as even the shortest available pulses satisfied it. This has changed spectacularly in recent years. Ultrashort, reproducible pulses have been generated at peak intensities of about 1 au, at various frequencies in the visible and near infrared, with pulse durations of less than 5 fs, and high repetition rates (see [11]). This means that, in few cycles, the intensity varies in the enormous range from 0 to 10^{16} W cm^{-2}. Of even more recent date is the generation of attosecond pulses [139, 140]. Note that the theoretical investigation of the effects of such short pulses on MPI and DS started long before they were produced experimentally.

If the adiabaticity condition required by single-state Floquet theory is not met, more terms need to be included in the expansion equation (23). This is the *'multistate Floquet theory'*, capable of covering the case of an arbitrary laser pulse. We now discuss the *interpretation of DS* based on it.

Let us assume that the frequency ω and the shape functions of the pulse are kept fixed in equation (16), and that the peak amplitude F_0 is increased starting from zero. For not too short pulses, or not too large F_0, such that $\mathrm{d}F_0(t)/\mathrm{d}t$ is small enough throughout the pulse, we are in a situation typically illustrated by our figures 3 and 4, for the 1D case, and by figures 5–8, for the 3D case. The evolution will be *adiabatic*, and the system will stay in one Floquet state, as discussed[24]. At some larger F_0, at times when $\mathrm{d}F_0(t)/\mathrm{d}t$ is large, the system will start feeling the turn-on of the pulse as a shock, and will make transitions to excited Floquet states; i.e., one or several coefficients $C_{v\neq 0}$ will become appreciable during the turn-on. This occurrence has been termed *'shake-up'*; we shall restrict the notion to the excitation of *discrete* excited Floquet states (excluding continuum ones). As a consequence, at the end of the pulse the system will have population in the field-free states associated with these Floquet states. Now, ionization from higher Floquet states has reduced rates, especially since all binding energies become smaller at high intensities (recall figure 1). Thus, more shake-up means smaller P_{ion}, so that DS will persist when increasing F_0. However, note that a *change in the physical nature of DS* has set in: from adiabatic (related to QS), to nonadiabatic (related to shake-up).

With growing F_0, $\mathrm{d}F_0(t)/\mathrm{d}t$ will become extremely large, and population will start to be transferred directly to the continuum during turn-on, spread evenly over a certain energy range. Consequently, expansion equation (23) will contain continuum Floquet states. Even in these states, multiphoton ('free–free') transitions occur, but the yields are smaller for higher electron energy. At turn-off, the atom suffers another shock, during which it may recapture some of this freely oscillating population, but much of it will end up in the continuum of the unperturbed atom, and will disperse. This effect we shall denote as *'shake-off'*. We are now dealing with a *change in the nature of the ionization*: from *multiphoton ionization*, involving absorption of photons, that can be described in terms of several discrete Floquet states and gives rise to well defined lines in the EPI/ATI electron spectrum, to *'shake-off' ionization*, caused by the shock of the field amplitude, that cannot be described in terms of discrete energy photons, and gives a continuous background to the EPI/ATI spectrum.

The realization that for pulses with very high peak field F_0 and extremely large $\mathrm{d}F_0(t)/\mathrm{d}t$ the electron oscillates practically freely and undergoes shake-off has led to the *'strong-field approximation' (SFA)*, used in a variety of forms (see, e.g., [151], and references therein): the electron wavepacket is assumed to evolve like that of a free particle during the whole pulse, having as initial condition the initial atomic state ψ_i. Let us denote by $\Psi^{(f)}(\boldsymbol{r},t)$ the free electron wavepacket evolving from ψ_i in the *absence* of the field. It is easy to show that, in the *presence* of the field, the wavepacket $\Psi^{(L)}(\boldsymbol{r},\tau)$ corresponding to the initial condition ψ_i

[24] The condition of adiabaticity poses a constraint on the magnitude of the matrix elements of the time derivative of the Hamiltonian $\partial H/\partial t$ (in our case the Floquet Hamiltonian), hence on $\mathrm{d}F_0(t)/\mathrm{d}t$; see e.g. [149, 150].

becomes in the length gauge, at the end of the pulse[25] τ,

$$\Psi^{(L)}(\boldsymbol{r},\,\tau) = \exp\left[-\mathrm{i}\frac{1}{2c^2}\int_0^\tau A^2\,\mathrm{d}t\right]\exp[\mathrm{i}(\delta\boldsymbol{p})_\tau\cdot\boldsymbol{r}]\Psi^{(f)}(\boldsymbol{r}-(\delta\boldsymbol{r})_\tau,\tau), \quad (25)$$

where $(\delta\boldsymbol{r})_\tau$ and $(\delta\boldsymbol{p})_\tau$ are the classical free-particle displacement and drift given by equation (17); for infinite-duration pulses, τ should be taken as ∞ (see section 3.1.2). If one deals with physical pulses, for which equations (18) and (19) are satisfied, SFA leads to the following ionization probability:

$$P_{ion}^{(SFA)} \simeq 1 - \sum_n |\langle\psi_n|\Psi^{(f)}(\boldsymbol{r},\tau)\rangle|^2. \quad (26)$$

Note that $P_{ion}^{(SFA)}$ is smaller than unity and no longer depends on F_0, which means that when equation (26) is applicable, DS has been attained. However, as the assumptions made in the derivation are rather drastic, equation (26) should be regarded as the limiting form of P_{ion} for extremely large F_0, at fixed τ (for a mathematical formulation of this, see section 3.3). Because of the spreading of the free-particle wavepacket $\Psi^{(f)}(\boldsymbol{r},t)$, the longer the effective pulse duration, the smaller the transition probabilities of discrete excitations will be, and the larger $P_{ion}^{(SFA)}$. The strong-field, short-pulse regime was investigated in the 1D case by Dörr *et al* [151], with an eye on possible applications of the short pulses produced recently [11]. (For the 1D case, see also the earlier work by Sonnenmoser [101].)

These conclusions are borne out by the numerical results for DS presented in section 3.1, which show that at short τ, P_{ion} manifests a plateau with respect to E_0 starting at several au, depending on ω; e.g., consider the 1D case of $\tau = 1$ in figure 4 [110] or the 3D case of $\tau_p = 0.25$ in figures 5–8 [136]. However, the plateau value equation (26) predicted by the SFA is attained very slowly, as shown for one dimension by Dörr *et al* [151], and confirmed for three dimensions by Dondera *et al* [135]. In these cases, the corresponding $(\delta\boldsymbol{r})_\infty$ and $(\delta\boldsymbol{p})_\infty$ are indeed zero, so that the application of equation (26) is warranted. On the other hand, if one of $(\delta\boldsymbol{r})_\infty$ and $(\delta\boldsymbol{p})_\infty$ is nonvanishing (and therefore increasing with F_0 at fixed envelope, according to equation (17)), the SFA result for P_{ion}, calculated with equation (25), increases to unity. This appears to be the case with the result in figure 3, where condition (19) is not satisfied.

Grobe and Fedorov [100] have shown that there is a limit to the times at which one can expect the true wavepacket $\Psi^{(L)}(\boldsymbol{r},t)$ to be represented adequately by the spreading free-particle wavepacket $\Psi^{(f)}(\boldsymbol{r},t)$. Indeed, at some time t^*, half the standard deviation $\Delta x(t)$ for $\Psi^{(f)}(\boldsymbol{r},t)$ will have grown to the point that it becomes equal to the excursion amplitude α_0: $\frac{1}{2}\Delta x(t^*) \approx \alpha_0$. For $t \gtrsim t^*$, the oscillating $\Psi^{(f)}(\boldsymbol{r},t)$ can also then overlap with the nucleus when at the turning points of its motion (where it has vanishing velocity), which yields a large probability for electron recapture. This implies that the true $\Psi^{(L)}(\boldsymbol{r},t)$ will then contain bound-state components, not accounted for by $\Psi^{(f)}(\boldsymbol{r},t)$.

3.3. Points of contention

Criticism has been raised in recent years regarding DS, based on the one hand on numerical computations, and on the other on mathematical physics.

[25] The result can be derived by passing ψ_i at $t = 0$ from the length to the velocity gauge (via the operator $\exp(\mathrm{i}\boldsymbol{A}(0)\cdot\boldsymbol{r}) = 1$), then propagating the wavepacket with $U(\tau) = \exp\{(-\mathrm{i}/2)\int_0^\tau[\boldsymbol{P} + (1/c)\boldsymbol{A}(t)]^2\,\mathrm{d}t\}$. Note that U contains the factor $\exp(-\mathrm{i}\boldsymbol{\alpha}(\tau)\cdot\boldsymbol{P})$ (see equation (2)) which has the effect of translating $\boldsymbol{r}$ into $\boldsymbol{r}+\boldsymbol{\alpha}(\tau)$, and the factor $\exp(-\mathrm{i}\,\boldsymbol{P}^2\tau/2)$, which implements free-particle propagation. By returning to the length gauge at the end of the pulse $t = \tau$, via the operator $\exp(-\mathrm{i}\boldsymbol{A}(\tau)\cdot\boldsymbol{r})$, and taking into account equation (17), one obtains wavefunction equation (25); see also Faria *et al* [102] Fring *et al* [104], Cycon *et al* [152].

On the *numerical side*, Geltman [114] has studied multiphoton ionization for the 1D delta-potential model, $V(x) = -B\delta(x)$, with only one bound field-free state. By applying his numerical methods, he did *not* find DS for flat-top pulses with $\sin^2$, or step-wise turn-on. Instead of a P_{ion} curve resembling those of figure 3, and displaying a DS branch, he found a P_{ion} growing to unity, and staying there (with slight oscillations). In [153] he expressed his views opposing stabilization.

The numerical result of [114] was disputed early on by Sonnenmoser [101], who did find evidence of DS for the same model. Somewhat later, Su *et al* [111] recalculated the problem under the same pulse conditions, and found a P_{ion} curve resembling the ones in figure 3, i.e. confirming the DS regime. In a recent comment on the latter calculation, Geltman agreed with all its results[26].

Mercouris and Nicolaides [115] attempted to resolve the dispute by applying their numerical method 'SSEA'. This resulted in a P_{ion} displaying *no* stabilization. The new contradiction prompted Dörr and Potvliege [113] to recalculate the problem; they did find DS, in close agreement with the results by Su *et al* [111].

On the *mathematical side*, rigorous results based on functional analysis have been obtained by Schrader, Fring, Kostrykin and Faria for the total ionization probability P_{ion} at the end of a laser pulse (see [102–104] and references therein). These were expressed as bounds on P_{ion}, on the one hand, and as limits of P_{ion}, on the other.

General formulae for both upper and lower *bounds on* P_{ion} were derived (denoted P_u and P_l, respectively) (see [102, section 3]). Obviously, $0 \leqslant P_l \leqslant P_{ion} \leqslant P_u \leqslant 1$. The formulae for P_l and P_u depend on the laser pulse via the two shifts $(\delta \boldsymbol{r})_\tau$ and $(\delta \boldsymbol{p})_\tau$, defined in equation (17). The formulae were then evaluated for n, l, m, states of H, and various forms of laser pulses. The investigation did not find evidence of DS, but did not contradict its existence, either. Indeed, no numerical calculation was signalled that violated the bounds. In fact this could hardly be possible, as both the mathematical-physics approach and the numerical integration proceed from TDSE. Obviously, numerical methods can never be exact, but the present computational capabilities allow a quite satisfactory treatment of one-electron ionization (programming errors excluded).

A different type of result was the derivation of *limits of* P_{ion} for a laser pulse $\boldsymbol{E}(t) = \boldsymbol{E}_0 g(t)$, where $E_0 \to \infty$, and $g(t)$ is a fixed function, nonvanishing only for $0 \leqslant t \leqslant \tau$. The function $g(t)$ is quite general (not necessarily oscillatory), and also covers the case of equation (16). It was shown (see [104], [102, section 4], [103]) that

$$\lim P_{ion} = \begin{cases} P_{ion}^{(SFA)} < 1, & \text{if equation (18) is satisfied,} \\ 1, & \text{otherwise,} \end{cases} \tag{27}$$

where $P_{ion}^{(SFA)}$ is given by equation (26). The first case allows for the possibility of atomic survival in a neutral state, while the second leads to complete ionization. Note that, from the experimental point of view, only the first case is possible, as discussed in connection with equation (18). These rigorous results substantiate the conclusions drawn from the SFA (equation (26)).

3.4. Classical approach

Soon after DS was discovered quantum mechanically, the question arose of whether it had a classical analogue. The idea of simulating ionization classically had already been successfully

[26] Geltman [112] still disagreed with the interpretation of the wiggles of the DS branch, as given by Su *et al* [108, 111]. His point of view was countered by Dörr and Potvliege [113].

applied to microwave ionization of highly excited Rydberg atoms (theory initiated by Leopold and Percival [154], see also [155]; experiments by Bayfield and Koch [156]). The principle of the method, known as 'classical-trajectory Monte Carlo simulation' or 'microcanonical-ensemble averaging', is the following (see, e.g., [157]). The initial condition (for example, the atomic ground state) is represented classically by a microcanonical ensemble in phase space, with the fixed energy $\epsilon_0 < 0$ of a quantum state (distribution function $\rho \propto \delta(\epsilon - \epsilon_0)$) and, in 3D calculations, having also fixed angular momentum L, and (sometimes) fixed projection of the angular momentum on the field axis, M. Thousands of phase-space points have been included in the ensemble. These were then allowed to evolve according to the classical equations of motion, and the analogues of the quantum averages were obtained by averaging over the ensemble at later times. The ionization probability P_{ion} at the end of a laser pulse was taken to be the fraction of trajectories having positive energies, i.e. escaping the vicinity of the atom. By analysing the dependence of P_{ion} on the peak field of the pulse, the existence of a classical stabilization could thus be ascertained. Recall that the classical dynamics of H in a monochromatic plane wave is invariant under the scaling of frequency ω, electric field amplitude E_0 and energy W, according to $\omega \Rightarrow n^{-3}\omega$, $E_0 \Rightarrow n^{-4}E_0$ and $W \Rightarrow n^{-2}W$, where n is a constant (assimilated in practice to the principal quantum number). Thereby, results for Rydberg states can be transposed to lower states (not necessarily in parameter ranges of interest, however), and vice versa. Hereafter we describe the NR work done; for more information on classical studies, see also the relativistic case in section 4.1.

The first application of the method to DS was made by Grohmalicki *et al* [158], for both 1D and 3D models. This was continued by the work by Gajda *et al* [159]. For the 1D model potential chosen, $V_s(x) = -(1 + x^2)^{-1/2}$, the results for P_{ion}, at the end of a pulse of sufficiently large peak field and sufficiently high frequency, displayed DS and considerable survival probability, in qualitative agreement with the quantal results by Su *et al* [2] (see our figure 3). Comparatively, quite small survival probability was found for the purely Coulomb 3D case, at peak intensities of several au (the survival was somewhat better for $L = 1$ than for 0). This was perceived to be in contradiction with the quantum mechanical results in [123] (pertaining, though, to different parameters), and a shortcoming of the classical approach. The authors remarked that, by introducing a soft-core 3D Coulomb potential $V_\epsilon(r) = -1/(r + \epsilon)$, where ϵ is of order unity, more survival could be achieved, comparable to that in the 1D case. However, later 3D quantal calculations (see section 3.1.2) have shown that DS is indeed much reduced in the 3D case in comparison to the 1D case, so that there is no reason to introduce the potential $V_\varepsilon(r)$. Rzażewski *et al* [160] have carried out a treatment of the two-electron problem with a 1D model along similar lines.

Ménis *et al* [161] studied both the 1D model potential $V_a(x) = -(a^2 + x^2)^{-1/2}$, where a was varied, and the true 3D Coulomb potential. In the 1D case, they found high sensitivity of P_{ion} to the value of the smoothing parameter a, namely, less atomic survival for smaller a. From this they concluded that soft-core Coulomb potentials were prone to be misleading. They also confirmed the reduced degree of stability in the 3D Coulomb case as compared to the 1D case, but cautioned against using soft-core potentials as overestimating DS.

Grobe and Law [162] studied the 1D model with potential V_s in the oscillating (KH) frame. They confirmed the existence of DS and explained, on the basis of the trajectories calculated, why ionization becomes classically difficult in intense fields. Bestle *et al* [163] have considered the same model with a suddenly turned on pulse of amplitude E_0 and duration τ_p. A systematic calculation of the dependence of P_{ion} on E_0 and τ_p again revealed DS.

The study of Benvenuto *et al*, pertaining to the 3D Coulomb case, emphasized the role of the angular momentum projection M on the field (at fixed L): case $M = 0$ was studied in [164], and case $M \neq 0$ in [165]. Their study was targeted at Rydberg microwave ionization, but the

results are more general due to the aforementioned scaling laws. Clear-cut DS was found for $M \neq 0$, but very little for $M = 0$ (at long pulse durations) (see figure 2 of [164]). The difference was interpreted as being due to the possibility, for $M = 0$, of the electron becoming close to the nucleus at large field amplitude, and ionizing. (Recall that DS is present in the quantum case for $M = 0$, see section 3.1.2, but at much shorter pulse durations than were considered here.) In a further publication by the same authors [166], a stability diagram in the energy–frequency plane was given, based on analytical estimates (see also Shepelyansky [167]). A criticism of classical results by others was presented.

Some calculations have compared directly the classical distribution probability in phase space with quantum phase-space quasiprobability distributions (such as the Wigner or Husimi distributions), that yield information basically equivalent to that of the wavefunction Ψ. An example is the work by Jensen and Sundaram [168, 169], who considered the case of an electron in the 1D potential V_a defined above, driven by a monochromatic plane wave. The classical dynamics were handled in the oscillating (KH) frame, based on the approximation of an electron 'periodically kicked' by the potential, which leads to the 'map approximation' of the dynamics in phase space. This allowed the identification of the stability regions of the motion at large field amplitudes (fixed points, periodic orbits etc), i.e. the existence of a classical stability against ionization. On the other hand, the quantal calculation of Floquet states and their Husimi distributions allowed the identification of some states strongly localized precisely near the classical fixed points. An explanation was advanced as to why the dichotomous structure of $|\Psi|^2$, found in the calculation by Su *et al* [2], had peaks spaced α_0 apart, instead of $2\alpha_0$ as required by HFFT (α_0 corresponds to the flat-top amplitude of their pulse). In a continuation of this work, Jensen and Sundaram [170] have extended their 1D analysis to the 3D Coulomb case, based again on the 'map approximation'. A stability diagram in the E_0, ω plane was derived, shown in their figure 1 (see also the discussion in [166]).

Later Watson *et al* [171] compared the microcanonical probability density with the Wigner quasiprobability for a 1D soft-core Coulomb model, in order to identify nonclassical effects *during* the evolution of a pulse. The pulse was chosen to have $\omega = 1$ au (a high-frequency case), a $\sin^2$ envelope of 24 cycles duration and peak field $E_0 = 10$ au. Their findings were interpreted in terms of the population in dressed KH states (see equation (21)). They found disagreement between the classical and quantum distributions for $t \lesssim 12$ cycles (but a signature of stabilization was nevertheless detected), and good agreement in the later part of the pulse ($t \gtrsim 12$ cycles), indicating that this stage could indeed be described classically.

More recently, Chism *et al* [118] have compared quantum mechanical and classical DS for a 2D model and circular polarization (see also section 3.1.1). Good correspondence was found between the stability regions in phase space, and the rotating, ring-shaped wavepacket.

These studies have indicated that atomic stabilization can be understood, up to a point, in classical terms, but that there are limitations. Specifically, the adiabatic pulse regime where quantum interference plays an important role cannot be covered (see the interpretation of QS in section 2.1.2), whereas nonadiabatic (shake-up/shake-off) manifestations of DS can. It should be mentioned that many of the classical studies were carried out at a time when the quantum mechanical picture was incomplete, so no proper quantitative comparison could be made. Consequently, a comprehensive picture of the connection between classical and quantum stabilization has yet to come.

4. Relativistic extensions

Atomic stabilization, in the QS and DS forms, was derived from NR dynamics. At the superintense fields at which it occurs, one might wonder whether NR dynamics can give a

trustworthy description of the phenomenon. In fact, it has been anticipated that relativity will have an adverse effect on the survival probability of the atom, and will destroy stabilization at some high intensity: stabilization is limited, therefore, to a window of intensities. The issue could be fully clarified by carrying out a relativistic calculation based on the Dirac equation. This has been precluded so far by the complexity of the numerical problem. The best one could do quantum mechanically to date was to study relativistic approximations, and models. The classical problem, however, has been treated fully relativistically.

Relativity comes into play in several ways: firstly, because in extremely intense fields the electron is driven with velocities close to the speed of light (classically: variation of mass with velocity becomes important). Secondly, the extended structure acquired by the atom due to the large excursion of the oscillating electrons forces the breakdown of the dipole approximation for the laser field; i.e., the propagation of the field within the atom (retardation) needs be taken into account. The vector potential of the field $\boldsymbol{A}(\boldsymbol{r}, t)$ is now a function also of $\boldsymbol{r}$, which leads to the appearance of the magnetic Lorentz force. Finally, relativity is needed for a consistent description of spin effects.

The expected order of magnitude of the retardation corrections is of the ratio of the magnetic Lorentz force to the electric force, i.e. $\mathcal{O}(v/c) = \mathcal{O}(eE_0 / mc\omega)$, where v is the average velocity of the electron quiver motion at small field $v = \mathcal{O}(\omega\alpha_0)$; note that the retardation corrections scale as E_0/ω. Relativistic dynamics corrections (classical variation of mass with velocity) are of order $(v/c)^2$. We shall be using in this section ordinary units.

4.1. Classical calculations

In the superintense fields we are concerned with, the electric force of the field is overwhelmingly dominant with respect to the Coulomb binding force, so that the latter can be ignored for most of the electron's motion. It is, therefore, useful to recall some facts about the relativistic motion of a free (unbound) electron.

To be specific, let us consider the case of a linearly polarized plane wave propagating in the positive Oz direction, with the $\boldsymbol{E}$ and $\boldsymbol{H}$ vectors oscillating along the Ox and Oy axes, respectively. The stationary free-electron motion is given in textbooks, e.g. [172]; see also Sarachik and Schappert [173, section 2]. In the field of a monochromatic plane wave, an electron with no drift velocity moves along a 'figure eight' trajectory in the O xz plane, with the axis of the 'eight' in the direction of the electric field[27], O x. The case of practical interest, however, is that of a free electron, initially at rest, acted upon by a finite-duration laser pulse propagating in the O z direction. In this case, the electron acquires a drift velocity in the Oz direction, that grows from zero to a maximum value, and then decreases back to zero (see, e.g., [173–175]). Although the electron is left at rest by the passing pulse (i.e. $(\delta \boldsymbol{p})_\tau = 0$, in the notation of section 3.1), its final position is displaced in the propagation direction (i.e. $(\delta z)_\tau \neq 0$), the displacement being larger for a longer pulse. When dealing with an atomic electron, the fact that $(\delta z)_\tau \neq 0$ will have a negative impact on the possibility that it will be recaptured by the atom at the end of the pulse (i.e. on the survival of the atom in a neutral state). The *destabilizing effect* of the relativistic shift $(\delta z)_\tau$ was pointed out by Katsouleas and Mori [177], as a caveat on NR stabilization calculations. A similar situation also occurs for arbitrary elliptic polarization.

Classical, fully relativistic Monte Carlo calculations were initiated before the discovery of stabilization by Kyrala [174], and pursued years later by Keitel and Knight [175]. The

[27] The 'width' and 'height' of the 'figure eight' (i.e. its extension in the direction of propagation and in the direction of electric field) tend to finite values as the field increases, the limit of their ratio being 0.18 (see [172]). At smaller intensities, the 'figure eight' collapses into a straight line segment along the O x axis, of length $2\alpha_0$ (twice the NR excursion).

latter found that (for short pulses) the classical ionization probability does manifest DS at high frequencies, such as $\omega = 5$ au, both with and without relativity, for $10 < E_0 \lesssim 100$ au. For $E_0 \gtrsim 100$ au, however, P_{ion} starts growing monotonically to unity in both cases, the growth in the relativistic case being considerably faster. In the NR case, the growth can be ascribed to the fact that the pulses used did not satisfy the first of conditions (18), the one leading to $(\delta \boldsymbol{r})_\tau = 0$ in NR dynamics (see also the quantal considerations in section 3.3). In the relativistic case, as noted above, the condition $(\delta \boldsymbol{r})_\tau = 0$ can never be satisfied, and hence the growth is unavoidable.

Kylstra *et al* [176] have carried out NR Monte Carlo simulations for a 2D model with a soft-core Coulomb potential, with short pulses at $\omega = 1$ and 2, to test the effects of retardation. On the one hand, these have confirmed the existence of NR classical DS, and the inhibiting effect of retardation on it. On the other hand, they have found good agreement when comparing to corresponding quantal calculations (see section 4.2.2), confirming the value of classical DS calculations.

4.2. Quantum calculations

4.2.1. Quasistationary stabilization. Relativistic HFFT. In the NR case it was possible to define a space translation of vector $\boldsymbol{\alpha}(t)$ (a unitary transformation), that eliminates the vector potential $\boldsymbol{A}(t)$ explicitly from the Schrödinger equation (3) and yields its space-translated form, equation (4). The latter is the starting point of the NR HFFT, described in section 2. The simplicity of the result is due to the fact that $\boldsymbol{A}$ was a function of t only, which no longer holds when retardation is included; e.g., for unidirectional propagation we have $\boldsymbol{A}(t - \boldsymbol{r} \cdot \boldsymbol{n}/c)$. For the case of a plane wave of arbitrary polarization, Krstic and Mittleman [178, 179], have, nevertheless, derived a unitary operator $\mathfrak{U}(\boldsymbol{r}, t)$, that eliminates the corresponding vector potential $\boldsymbol{A}$ from the Dirac equation while changing the atomic potential $V(\boldsymbol{r})$ into $\tilde{V}(\boldsymbol{r}, t) \equiv \mathfrak{U}\, V(\boldsymbol{r})\, \mathfrak{U}^{-1}$. The transformed equation is exact, but the difficulty with $\tilde{V}(\boldsymbol{r}, t)$ is that it is an *integral* matrix operator. However, they have shown that in the case of a light atom, where only NR internal momenta are involved, $\tilde{V}(\boldsymbol{r}, t)$ reduces to a *local* matrix operator. If spin terms are neglected, this is just a multiplicative potential $\tilde{V}_P(\boldsymbol{r}, t)$. $\tilde{V}_P(\boldsymbol{r}, t)$ is the relativistic extension of the NR oscillating potential $V(\boldsymbol{r} + \boldsymbol{\alpha}(t))$. At high frequencies, the equation obtained can be handled by the procedures of the NR HFFT.

Krstic and Mittleman have made the first step in this direction, and have derived a *relativistic high-frequency structure equation*, generalizing equation (6); it contains $\tilde{V}_P^{(0)}(\boldsymbol{r}, \alpha_0, \omega)$, the cycle-averaged form of $\tilde{V}_P(\boldsymbol{r}, t)$. Note that $\tilde{V}_P^{(0)}(\boldsymbol{r}, \alpha_0, \omega)$ depends on α_0, as well as on ω; it is logarithmically singular along the relativistic path of the free classical electron. For linear polarization, this path is the aforementioned 'figure eight'. The structure of the averaged potential $\tilde{V}_P^{(0)}(\boldsymbol{r}, \alpha_0, \omega)$ was analysed by Ermolaev [180]. The Krstic–Mittleman structure equation has not been solved for realistic 3D cases so far, but a 1D model with a soft, quasi-Coulomb potential was discussed by Ermolaev [180]. The ground-state energy eigenvalue $W_0^{(R)}(\alpha_0, \omega)$ shows at large α_0 considerable departure from its NR counterpart, $W_0^{(NR)}(\alpha_0)$. However, for reasonably large E_0 (e.g. $E_0 < 100$ au), the deviation of the relativistic curves from $W_0^{(NR)}(\alpha_0)$, given by figure 1 of [180], is quite small. No ionization rates were calculated, and hence no information was obtained on how relativity may affect NR QS.

Soluble models. Faisal and Radożycki [181, 182], have developed a relativistically soluble model for a 'separable' pseudopotential of the form $V(r) = V_0 |\phi(r)\rangle\langle\phi(r)|$ (a projection operator on the unique bound state $|\phi(r)\rangle$). The equation solved was the (spinless) Klein–Gordon equation. With a circularly polarized monochromatic field, the Floquet quasienergy of the ground state can be obtained from an integral equation (as in the corresponding NR

case [79, 80]). This was solved at low frequencies, and QS was shown to exist under certain circumstances.

Full Floquet calculations. Potvliege [183] has carried out an NR Floquet calculation with retardation included for the circular state 5g ($m = 4$) of H (this was the initial state chosen for the stabilization experiments described in section 5). The goal was to check for possible departures from the dipole approximation rate calculated by Piraux and Potvliege [133]. No departure was found in the range of up to 4×10^{14} W cm^{-2}, covering the experiment.

4.2.2. Dynamic stabilization. As concerns DS, one has studied the effect of retardation corrections (i.e. of the magnetic Lorentz force) on the NR dipole approximation results for P_{ion}. The early 3D work by Bugakov *et al* [184] has retained only some of the retardation corrections. At $\omega = 2$ au, for a Gaussian pulse envelope of $\tau_p = 5$ cycles duration (as defined by equation (20)), the retardation corrections found for peak fields $E_0 < 10$ au were negligible (see [184, figure 2(a)]); their result agrees at the graphical level with the NR calculations shown in our figure 6. For $E_0 > 10$ au, on the other hand, their NR dipole approximation result differs drastically from figure 6. Latinne *et al* [127] have taken into account retardation in three dimensions fully, using a pulse with linear turn-on (but no turn-off), and various peak intensities. Negligible retardation corrections were found for peak fields $E_0 < 16$ au at $\omega = 2$, and for $E_0 < 40$ au at $\omega = 5$ au.

More recently, Kylstra *et al* [176] and Vázquez de Aldana *et al* [185] have fully included retardation in an NR 2D model calculation with a soft-Coulomb potential, and trapezoidal pulses of 12 cycles duration. The results for P_{ion}, calculated with or without retardation, start deviating from each other abruptly at about $E_0 = 9$ for $\omega = 1$, but for $\omega = 2$ they are still in good agreement at $E_0 = 18$ au, the maximum field strength considered (see figure 1 of [176]). Thus, a large part of the NR DS regime lies well within the range of intensities for which retardation (and other relativistic) corrections are negligible. In [185], also the effects of the pulse duration on the limitations of the dipole result were analysed. Moreover, the possibility was explored that, by placing the atom in a standing wave at a node of the magnetic field, the inhibiting effect of retardation on DS might be reduced, but this has not proven to be the case. Rather similar results on the role of retardation on DS have been obtained by Ryabikin and Sergeev [186, 187]. Some of the results in these papers were assessed by Joachain and Kylstra [188].

Taïeb *et al* [189] have considered a relativistic 1D model with soft-core Coulomb potential, brought into the stabilization regime by high-frequency superintense radiation. By applying a second field, of relatively low frequency and intensity, and by comparing the NR and relativistic ATI spectra, notable signatures of relativity were found.

5. Experiments

Two independent, state-of-the-art experiments have been carried out, stimulated by the theoretical work on QS of low-lying Rydberg states [39]. The most favourable candidate under the prevalent experimental circumstances was considered to be the Ne atom, and the circular state 5g ($n = 5$, $l = m = 4$) was selected as the test case. The first experiment, by de Boer *et al* [3], involved two stages: the preparation of the initial Rydberg state, and the detection of its ionization by an intense laser field of (relatively) high frequency. In the second experiment, by van Druten *et al* [4], a third stage was added to monitor the population left in the Rydberg state. The second experiment confirmed the first one; we shall present the latter in the following.

The ionized electrons were detected with the help of the 'magnetic bottle' electron spectrometer. The apparatus consists of an ionization chamber connected to a flight tube, having an inhomogeneous magnetic field applied along its axis. The field is considerably

stronger at the laser focus than in the flight tube, with the effect that the ionized electron trajectories are parallelized to the axis of the flight tube and guided towards a multi-channel plate detector placed at its end, which energy-analyses them according to their time of flight.

The three stages of the experiment used different laser pulses. These were shone successively into the ionization chamber filled with Ne, in a direction perpendicular to the axis of the flight tube (i.e. to the direction of the magnetic field). The first pulse, the 'preparation pulse', consisted of intense circularly polarized UV light ($\omega_1 = 4.34$ eV, pulse duration 1 ps, $I \approx 200\,\mathrm{TW\,cm^{-2}}$). Its role was to populate the 5g state. The second, the 'main pulse', was the one driving the ionization to be stabilized. It consisted of red light ($\omega_2 = 2.0\,\mathrm{eV} = 0.073$ au), was of short duration (90 fs) and intense ($I \leqslant 230\,\mathrm{TW\,cm^{-2}}$), and was linearly polarized. It could be delayed by a variable time τ_d with respect to the preparation pulse. The high-frequency condition (9) is relatively well satisfied for the ω_2 photons and the $m = 4$ manifold, to which the initial states belonged, whose largest binding energy is $W^{(4)} = 0.02$ au: $\omega_2 > W^{(4)}$ (see section 2.1.2). Finally, the 'probe pulse' consisted of green light ($\omega_3 = 2.33$ eV) of low intensity ($I \leqslant 10\,\mathrm{GW\,cm^{-2}}$). Its duration was long (5 ns) and it was weakly focused and had sufficiently high fluence to ionize all the population left in the 5g and neighbouring states. It was delayed by 14 ns with respect to the preparation pulse. Its role was to probe the population left in the 5g state after applying the first two pulses.

The excited $(2p^5)5g$ state was produced from the ground state $2p^6$ of Ne by the absorption of five photons from the preparation pulse. In the one-electron approximation, this corresponds to a transition from the $(2p, m_l = -1)$ orbital to $(5g, m_l = 4)$. The magnetic quantum numbers are referred to the axis of propagation of the preparation beam. At vanishing field, five photons are barely sufficient to access the continuum. However, there is a large increase in the ionization potential of the ground state during the turn-on of the field (primarily due to the quiver energy gained), which means that the ground-state level is shifted downwards with respect to the continuum, whereas the Rydberg states remain close to it in energy. Consequently, the location of the five-photon resonance from the ground state sweeps through the (n, g)-Rydberg series during the turn-on. Population is transferred to these states in the process (but also to the continuum), and a large fraction of it survives the preparation pulse, so that it can be used as initial population for the main pulse. However, along with the 5g states, the 6g, 7g etc states are also populated to a lesser extent. It was extremely difficult to produce sufficient 5g population, so that the optimization of this stage was essential for the success of the experiment.

In high-intensity experiments, there is always a spatial distribution of peak intensities in the focal region, which substantially complicates the interpretation of the results. This difficulty was circumvented by arranging that the focal region of the preparation pulse (containing the excited atoms) be much tighter than that of the overlapping focal region of the main pulse. Moreover, by arranging that the focal region of the preparation pulse be at the centre of the main focal region, excited atoms were produced only in that part of the latter which contains the peak intensities. On the other hand, the fact that the preparation- and main-pulse beams were parallel created a problem: the axis of quantization of the magnetic states prepared by the first beam was perpendicular to the direction of linear polarization of the main beam (chosen to be also perpendicular to the magnetic field), instead of being parallel to it as required by the theory. A remarkably ingenious solution was give to this problem, by making use of the magnetic field of the electron spectrometer, which is perpendicular to the (parallel) beams. In this field, the $m = 4$ excited atoms undergo Larmor precession, which rotates their axis of quantization around the direction of the magnetic field, allowing it to become perpendicular to the beam direction after a quarter of a Larmor period. By sending in the main pulse with this time delay ($\tau_d = 20$ ps), the axis of quantization of the atoms will rotate and become parallel to the direction of polarization of the main pulse, as needed.

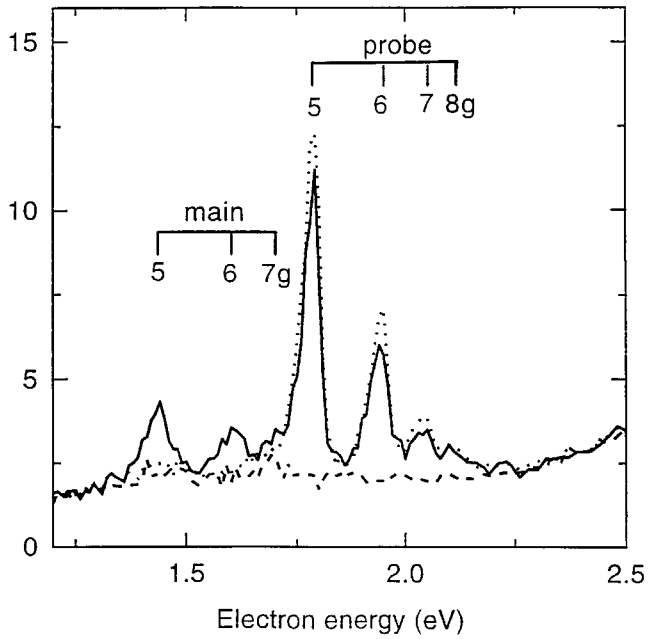

Figure 10. Adiabatic stabilization experiment by van Druten *et al* [4] on the Rydberg states of Ne. The solid curve shows the photoelectron spectrum after the three laser pulses (preparation, main and probe) have been applied (see text). The expected energies of electrons ionized from the $(2p)^5ng$ states by the main and probe pulses are marked.

A typical electron spectrum for the case where all three pulses were applied successively is shown in figure 10 (solid curve). The peaks represent one-photon absorptions from the different n, g states populated by the preparation pulse. There are two superposed series of peaks: one due to the main pulse, the other to the probe pulse (as indicated). The energy difference of peaks corresponding to the same state is $\omega_3 - \omega_2 = 0.33$ eV. The figure also contains a dashed curve, representing the spectrum with the probe laser *off*, for $\tau_d = -5$ ps. (Negative τ_d means that the main pulse precedes the preparation pulse.) Thus, the dashed curve represents the electron yield from the *ground state* due to the main and preparation pulses, i.e. gives the background signal under the peaks of the main pulse in figure 10. By subtracting the dashed curve from the full curve under the main photon peaks in figure 10, one could determine the fraction of the $(2p)^5$5g population that has ionized. Figure 10 also contains a dotted curve, giving the spectrum with the probe laser *on*, but with $\tau_d = -5$ ps. This yields the total population generated in the $(2p)^5$5g state (all of which is ionized), in the presence of the background from the ground state due to the main and preparation pulses. By subtracting the full curve from the dotted one under the probe-photon peaks, one could directly determine the fraction of the $(2p)^5$5g population that has survived the main pulse.

The fractions of the $(2p)^5$5g surviving and ionized populations are shown in figure 11, with an error bar on the results. Note first that, within the error shown, the two fractions add to unity, indicating that there are no other significant decay channels than one-photon ionization. This agrees with the theoretical prediction made in section 2.1.2, regarding the dominance of one-photon ionization at high frequencies. Next, at peak intensities of the main pulse higher than approximately 60 TW cm^{-2}, practically no ionization is observed. The surviving population stabilizes at about 70% of its initial value, and conversely, some 30% gets ionized. These

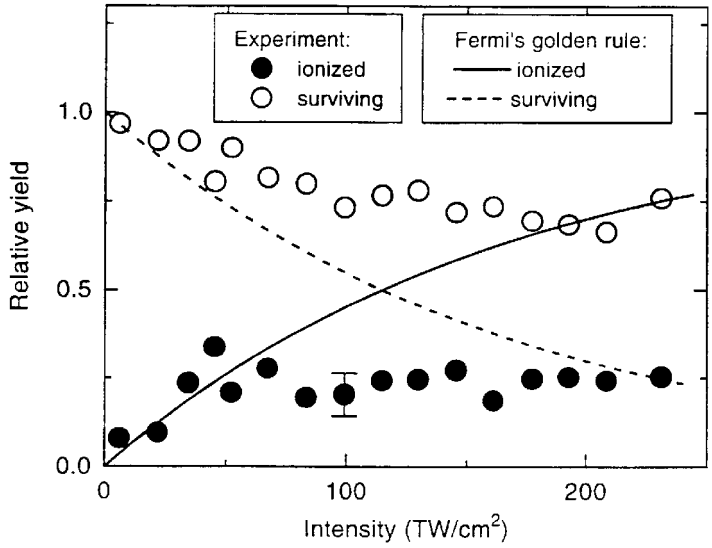

Figure 11. Stabilization experiment by van Druten *et al* [4]. Measured fraction of ionized (open circles), and surviving (solid circles) populations in the $(2p)^5 5g$ state of Ne following exposure to the main pulse (inducing stabilization), versus main-pulse intensity. Drawn curves represent populations according to LOPT ('Fermi's golden rule'): ionized fraction (solid curve), surviving fraction (dashed curve).

results disagree with LOPT, represented in figure 11 by the drawn curves, and are a clear-cut indication of DS.

A quantitative *theoretical analysis* of the experiment was made by Piraux and Potvliege [133]. They evaluated the ionization probability at the end of the pulse under the conditions of the experiment, both in the adiabatic approximation (calculating Γ from Floquet theory and using equation (24)) and dynamically, by integrating TDSE. Several pulse shapes were explored ($\sin^2$, sech). Identical results for P_{ion} were found for the same pulse shape with both methods, showing the fully adiabatic character of the atomic evolution considered. DS was confirmed. The results for P_{ion} calculated with the sech pulse were in fair quantitative agreement with experiment (see figure 3 of [133]). As mentioned already, in order to check the validity of the previous dipole approximation results for Γ, Potvliege [183] has carried out a Floquet calculation fully including retardation; no difference was found up to 4×10^{14} W cm^{-2} (the range of experimental interest).

The above experiment was aimed at determining yields (i.e. P_{ion}) and was conducted under adiabatic conditions of atomic evolution; under the circumstances, DS is a manifestation of the underlying existence of QS (see equation (24)). As a matter of conceptual interest, we mention that one can devise ways for ascertaining the existence of QS directly. One such possibility would be to apply an intense adiabatic pulse with a flat top, and to monitor the exponential decay of an initial atomic population during the flat top. Whereas this procedure has often been applied theoretically to obtain Γ from wavepacket calculations (e.g. [123, 135]), it could be implemented experimentally too. For example, by applying a pulse of the kind mentioned, the decay of the initial state of the population could be monitored by a low-intensity, auxiliary pulse, that fully depletes the remaining population, and is triggered at successive instants. Although not easy, the experiment should be feasible (private communication from H G Muller).

6. Conclusion and perspectives

From the work reviewed, one may conclude that the decade of research on superintense-field stabilization has firmly established the concept theoretically and experimentally, and that its physics has been by and large understood. Notwithstanding, challenging *open problems* exist. We give some examples here, starting with experimental ones.

Ground-state DS for atoms with large ionization potentials (such as H, noble gas atoms) has been identified early on as an important goal of research, both for its fundamental interest and for its potential applications. Now theoretically under control for one-active-electron systems, DS was until very recently completely out of experimental reach, for lack of adequate lasers. Promising prospects have opened up with the advent of intense high-frequency light sources. For example, VUV-FELs have been built and are now in test operation (HASYLAB at DESY), or under construction (BNL). Photon energies in excess of 200 eV, at high intensities (10^{18} W cm^{-2} and up), should soon become available at HASYLAB. Technical studies have indicated that the pulse lengths could be brought down to some 30 fs by advanced manipulation of the electron beam, but they would still not be at the femtosecond level required for ground-state DS. Nevertheless, by seeding with XUV radiation and use of chirped pulse amplification, it should be possible to further reduce the pulse length and bring it down into the desired range. A different prospect is the use of attosecond pulses recently produced by high harmonic generation. Techniques are now being developed for their handling; a tight focusing can lead to some 100 au of intensity, at several au of photon energy. In both cases, the DS experiment would need to be state of the art.

Short-pulse DS. The experiments so far have been done with pulses in the adiabatic regime. Now that very short pulses (FWHM of several cycles) have become available, it is of interest to explore experimentally the other mechanisms responsible for DS, shake-up and shake-off. This could be also done with low-frequency laser sources in the case of excited states of H, or ground states of atoms with small ionization potentials such as alkalis.

Observation of QS. The study of P_{ion} is an indirect way to confirm QS. A direct possibility would be to monitor the exponential decay of some initial atomic population during the flat top of an intense adiabatic pulse. Various monitoring schemes can be imagined. While not easy, the experiment should be feasible.

Atomic distortion. Stabilization is coupled to extreme (polarization-dependent) atomic distortion, a fact well documented theoretically in the high-frequency regime. The possibility arises, therefore, that atomic structure could be (transiently) tailored for use in other (adequately synchronized) experiments.

Exotic systems have been predicted, like hydrogen multiple-negative ions (a proton binds more than two electrons, not possible in the field-free limit). Theoretically predicted at high frequencies and intensities, such structures are in the DS regime, and already relatively stable at their appearance. H^{2-} (a proton plus three electrons) is in principle within experimental reach.

Other problems require further investigation of their theoretical basis. Examples follow.

Role of frequency. QS and DS have been studied theoretically primarily in the high-frequency regime. Little is known about the possibility and conditions of occurrence of stabilization at *low* frequencies. Moreover, it is known that at low frequencies 'light-induced atomic states' (LIS) appear at high intensities. These are, from the start, in the high-frequency regime and therefore undergo QS. Their excitation might allow for a new avenue of manifestation of DS.

Pulse shape effects. It has been recognized in theoretical 1D studies that the shape of the pulse envelope is of considerable consequence for DS and atomic survival. Indeed, it was shown that the atom evolves towards high intensities along so-called 'diabatic Floquet paths',

consisting of sequences of Floquet states. The possibility thus appears of steering the evolution along diabatic paths that have maximum atomic survival, by adequate pulse shaping ('quantum control').

Relativistic effects. Their theoretical study has been stimulated by the superintense fields available at low frequencies, and has started to reveal new exotic behaviour. Computational limitations are still a handicap here. The extension of the stabilization 'window' (i.e. of the intensity range in which NR DS remains valid) is of great interest.

The problems listed above refer to the case of one-active-electron atoms, but some of them can be extended to *two-electron atoms* (H^- or He), or *simple molecules* (H_2^+, H_2 etc). Because of the increased number of degrees of freedom, new problems appear. Thus, what is the effect of electron correlation on the single-active-electron results for stabilization (QS and DS)? Does DS exist beyond the one-active-electron approximation? In the context of several electrons, the notion of 'high frequency' becomes uncertain: to which of the several ionization potentials should ω be compared? Moreover, more complex forms of stabilization have been suggested.

Many more problems are open; superintense-field stabilization has rewarding research to offer in the years to come.

Acknowledgments

The author would like to acknowledge instructive discussions with Harm G Muller. He has greatly enjoyed the stimulating atmosphere at ITAMP, where much of this work was done, and in particular his amiable interaction with Alex Dalgarno. Support from the I R Foundation is gratefully acknowledged. He also thanks N Kylstra and H G Muller for permission to reproduce their figures.

References

[1] Pont M and Gavrila M 1990 *Presented at SILAP I (Rochester, NY, June 1989) Phys. Rev. Lett.* **65** 2362
[2] Su Q, Eberly J H and Javanainen J 1990 *Phys. Rev. Lett.* **64** 862
[3] de Boer M P, Hoogenraad J H, Vrijen R B, Constantinescu R C, Noordam L D and Muller H G 1993 *Phys. Rev. Lett.* **71** 3263
de Boer M P, Hoogenraad J H, Vrijen R B, Constantinescu R C, Noordam L D and Muller H G 1994 *Phys. Rev.* A **50** 4085
[4] van Druten N J, Constantinescu R, Schins J M, Nieuwenhuize H and Muller H G 1997 *Phys. Rev.* A **55** 622
[5] Freeman R R and Bucksbaum P H 1991 *J. Phys. B: At. Mol. Opt. Phys.* **24** 325
[6] Freeman R R, Bucksbaum P H, Cooke W E, Gibson G, McIlrath T J and van Woerkom L D 1992 *Atoms in Intense Laser Fields* ed M Gavrila (New York: Academic) p 43
[7] Burnett K, Reed V C and Knight P L 1993 *J. Phys. B: At. Mol. Opt. Phys.* **26** 561
[8] DiMauro L F and Agostini P 1995 *Adv. At. Mol. Opt. Phys.* **35** 79
[9] Protopapas M, Keitel C H and Knight P L 1997 *Rep. Prog. Phys.* **60** 389
[10] Joachain C J, Dörr M and Kylstra N J 2000 *Adv. At. Mol. Opt. Phys.* **42** 225
[11] Brabec T and Krausz F 2000 *Rev. Mod. Phys.* **72** 545
[12] Mourou G A, Barty C P J and Perry M D 1998 *Phys. Today* 22
[13] Gavrila M 1992 *Atoms in Intense Laser Fields* ed M Gavrila (New York: Academic) p 435
[14] Eberly J H and Kulander K C 1993 *Science* **262** 1229
[15] Delone N B and Krainov V P 1995 *Usp. Fiz. Nauk* **165** 1295 (Engl. transl. 1995 *Sov. Phys.–Usp.* **38** 1247)
[16] Muller H G 1996 *Super-Intense Laser–Atom Physics* vol 4, ed H G Muller and M Fedorov (Dordrecht: Kluwer) p 1
[17] Gavrila M 2000 *Multiphoton Processes (AIP Conf. Proc. vol 525)* ed L DiMauro, R R Freeman and K C Kulander (New York: American Institute of Physics) p 103
[18] Lankhuijzen G M and Noordam L D 1997 *Adv. At. Mol. Opt. Phys.* **38** 121
[19] Gallagher T F 1994 *Rydberg Atoms* (Cambridge: Cambridge University Press)

[20] Pauli W and Fierz M 1938 *Nuovo Cimento* **15** 167
[21] Kramers H A 1956 *Collected Scientific Papers* (Amsterdam: North-Holland)
[22] Henneberger W C 1968 *Phys. Rev. Lett.* **21** 838
[23] Faisal F H 1973 *J. Phys. B: At. Mol. Phys.* **6** L89
[24] Schweber S S 1994 *QED and the Men Who Made It* (Princeton, NJ: Princeton University Press)
[25] Manakov N L, Ovsiannikov V D and Rapoport L P 1986 *Phys. Rep.* **141** 319
[26] Chu S I 1985 *Adv. At. Mol. Phys.* **21** 197
Chu S I 1989 *Adv. Chem. Phys.* **73** 739
[27] Potvliege R M and Shakeshaft R 1992 *Atoms in Intense Laser Fields* ed M Gavrila (New York: Academic) p 373 section 12
[28] Burke P G, Francken P and Joachain C J 1991 *J. Phys. B: At. Mol. Opt. Phys.* **24** 751
[29] Moiseyev N 1998 *Phys. Rep.* **302** 211
[30] Gavrila M and Kaminski J Z 1984 *Phys. Rev. Lett.* **52** 614
[31] Gersten J and Mittleman M H 1976 *J. Phys. B: At. Mol. Phys.* **9** 2561
[32] Pont M 1989 *Phys. Rev.* A **40** 5659
[33] Gavrila M 1985 *Fundamentals of Laser Interactions (Springer Lecture Notes in Physics vol 229)* ed F Ehlotzky (Berlin: Springer) p 3
[34] Marinescu M and Gavrila M 1996 *Phys. Rev.* A **53** 2513
[35] Wells J C, Simbotin I and Gavrila M 1997 *Laser Phys.* **7** 525
Wells J C, Simbotin I and Gavrila M 1997 *Phys. Rev.* A **56** 3961
[36] Martin P A and Sassoli de Bianchi M 1995 *J. Phys. A: Math. Gen.* **28** 2403
[37] Pont M, Walet N R, McCurdy C W and Gavrila M 1988 *Phys. Rev. Lett.* **61** 939
[38] Pont M, Walet N R and Gavrila M 1990 *Phys. Rev.* A **41** 477
[39] Vos R J and Gavrila M 1992 *Phys. Rev. Lett.* **68** 170
[40] Shertzer J, Chandler A and Gavrila M 1994 *Phys. Rev. Lett.* **73** 2039
[41] Muller H G and Gavrila M 1993 *Phys. Rev. Lett.* **71** 1693
[42] Perez C, Lefebvre R and Atabek O 1997 *J. Phys. B: At. Mol. Opt. Phys.* **30** 5157
Perez C, Lefebvre R and Atabek O 1998 *J. Phys. B: At. Mol. Opt. Phys.* **31** 4513
[43] Bardsley J N and Comella M J 1989 *Phys. Rev.* A **39** 2252
[44] Yao G and Chu S I 1992 *Phys. Rev.* A **45** 6735
[45] Grozdanov T P, Krstic P S and Mittleman M H 1990 *Phys. Lett.* A **149** 144
[46] Sanpera A, Su Q and Roso-Franco L 1993 *Phys. Rev.* A **47** 2312
[47] Boca M, Chirila C, Stroe M and Florescu V 2001 *Phys. Lett.* A **286** 410
[48] Potvliege R M 2000 *Phys. Rev.* A **62** 013403
[49] Ben-Tal N, Moiseyev N and Kosloff R 1993 *J. Chem. Phys.* **96** 9610
[50] Dörr M, Potvliege R M, Proulx D and Shakeshaft R 1991 *Phys. Rev.* A **43** 3729
[51] Wiedemann H 1994 *Phys. Rev.* A **50** 2769
[52] Fearnside A S, Potvliege R M and Shakeshaft R 1995 *Phys. Rev.* A **51** 1471
[53] Wells J C, Simbotin I and Gavrila M 1998 *Phys. Rev. Lett.* **80** 3479
Wells J C, Simbotin I and Gavrila M 1999 *Phys. Rev. Lett.* **82** 665
[54] Lefebvre R, Stern B and Atabek O 1999 *J. Phys. B: At. Mol. Opt. Phys.* **32** 3271
[55] Dörr M, Burke P G, Joachain C J, Noble C J, Purvis J and Terao-Dunseath M 1993 *J. Phys. B: At. Mol. Opt. Phys.* **26** L275
[56] Lefebvre R and Stern B 2001 *Int. J. Quantum Chem.* **84** 552
[57] Cheng T, Liu J and Chen S 1999 *Phys. Rev.* A **59** 1451
Cheng T, Liu J and Chen S 2000 *Phys. Rev.* A **62** 033402
[58] Lambropoulos P 1985 *Phys. Rev. Lett.* **55** 2141
[59] Pont M and Shakeshaft R 1991 *Phys. Rev.* A **44** R4110
[60] Baik M G, Pont M and Shakeshaft R 1995 *Phys. Rev.* A **51** 3117
[61] Potvliege R M and Smith P H G 1993 *Phys. Rev.* A **48** R46
[62] Scrinzi A, Elander N and Piraux B 1993 *Phys. Rev.* A **48** R2527
[63] Mittleman M H 1990 *Phys. Rev.* A **42** 5645
[64] Gavrila M and Shertzer J 1996 *Phys. Rev.* A **53** 343
[65] van Duijn E, Gavrila M and Muller H G 1996 *Phys. Rev. Lett.* **77** 3759
[66] van Duijn E and Muller H G 1996 *Phys. Rev.* A **56** 2182
van Duijn E and Muller H G 1996 *Phys. Rev.* A **56** 2192
[67] Potvliege R M and Shakeshaft R 1989 *Phys. Rev.* A **40** 3061
[68] Potvliege R M 1999 *Phys. Rev.* A **60** 1311

[69] Burke P G, Francken P and Joachain C J 1990 *Europhys. Lett.* **13** 617
[70] Dimou L and Faisal F H M 1993 *Laser Phys.* **3** 440
[71] Giusti-Suzor A and Zoller P 1987 *Phys. Rev.* A **11** 5178
[72] Dimou L and Faisal F H M 1992 *Phys. Rev.* A **46** 4442
[73] Dimou L and Faisal F H M 1994 *Phys. Rev.* A **49** 4564
[74] Marte P and Zoller 1991 *Phys. Rev.* A **43** 1512
[75] Peshkin U and Moiseyev N 1993 *J. Chem. Phys.* **99** 4590
Peshkin U and Moiseyev N 1994 *Phys. Rev.* A **49** 3712
[76] Millack T 1993 *J. Phys. B: At. Mol. Opt. Phys.* **26** 4777
[77] Zakrzewski J and Delande D 1995 *J. Phys. B: At. Mol. Opt. Phys.* **28** L667
[78] Buchleitner A and Delande D 1993 *Phys. Rev. Lett.* **71** 3633
[79] Berson I J 1975 *J. Phys. B: At. Mol. Phys.* **8** 3078
[80] Manakov N L and Rapoport L P 1975 *Zh. Eksp. Teor. Fiz.* **68** 842 (Engl. transl. 1976 *Sov. Phys.–JETP* **42** 430)
[81] Faisal F H M, Filipowicz P and Rzażewski K 1990 *Phys. Rev.* A **41** 6176
[82] Krstic P S, Milosevic D B and Janev R K 1991 *Phys. Rev.* A **44** 3089
[83] Filipowicz P, Faisal F H M and Rzażewski K 1991 *Phys. Rev.* A **44** 2210
[84] LaGattuta K J 1994 *Phys. Rev.* A **49** 1745
[85] Krainov V P and Preobrazhenskii M A 1993 *Zh. Eksp. Teor. Fiz* **103** 1143
(Engl. transl. 1993 *Sov. Phys.–JETP* **76** 559)
[86] Manakov N L, Frolov M V, Borca B and Starace A F 2001 *Super-Intense Laser–Atom Physics (Proc. SILAP VI)* ed B Piraux and K Rzażewski (Dordrecht: Kluwer) p 295
[87] Kaminski J Z 1995 *Phys. Rev.* A **52** 4976
[88] Gersten J and Mittleman M H 1974 *Phys. Rev.* A **10** 74
[89] Gersten J and Mittleman M H 1975 *Phys. Rev.* A **11** 1103
[90] Reiss H R 1980 *Phys. Rev.* A **22** 1786
[91] Reiss H R 1992 *Phys. Rev.* A **46** 391
[92] Su Q and Eberly J H 1992 *Laser Phys.* **2** 598
[93] Wells J C, Simbotin I and Gavrila M 2002 in preparation
[94] Millack T, Véniard V and Henkel J 1993 *Phys. Lett.* A **176** 433
[95] Moiseyev N and Cederbaum L S 1999 *J. Phys. B: At. Mol. Opt. Phys.* **32** L279
[96] Ivanov M Yu, Tikhonova O V and Fedorov M V 1998 *Phys. Rev.* A **58** R793
[97] Fedorov M V and Movsesian A M 1988 *J. Phys. B: At. Mol. Opt. Phys.* **21** L155
[98] Fedorov M V 1993 *Laser Phys.* **3** 219
[99] Fedorov M V and Tikhonova O V 1998 *Phys. Rev.* A **58** 1322
[100] Grobe R and Fedorov M V 1992 *Phys. Rev. Lett.* **68** 2592
Grobe R and Fedorov M V 1993 *J. Phys. B: At. Mol. Opt. Phys.* **26** 1181
[101] Sonnenmoser K 1993 *J. Phys. B: At. Mol. Opt. Phys.* **26** 457
[102] Faria C F M, Fring A and Schrader R 1999 *Laser Phys.* **9** 379
[103] Faria C F M, Fring A and Schrader R 2000 *Multiphoton Processes (AIP Conf. Proc. vol 525)* ed L DiMauro, R P Freeman and K C Kulander (New York: American Institute of Physics) p 150
[104] Fring A, Kostrykin V and Schrader R 1997 *J. Phys. A: Math. Gen.* **30** 8599
[105] Eberly J H, Grobe R, Law C K and Su Q 1992 *Atoms in Intense Laser Fields* ed M Gavrila (New York: Academic) p 301
[106] Su C K 1993 *Laser Phys.* **2** 241
[107] Wiedemann H, Mostowski J and Haake F 1994 *Phys. Rev.* A **49** 1171
[108] Su Q, Irving B P and Eberly J H 1997 *Laser Phys.* **7** 1
[109] Florescu A, Wells J C and Gavrila M unpublished
[110] Patel A, Kylstra N J and Knight P L 1999 *J. Phys. B: At. Mol. Opt. Phys.* **32** 5759
[111] Su Q, Irving B P, Johnson C W and Eberly J H 1996 *J. Phys. B: At. Mol. Opt. Phys.* **29** 5755
[112] Geltman S 1999 *J. Phys. B: At. Mol. Opt. Phys.* **32** 853
[113] Dörr M and Potvliege R M 2000 *J. Phys. B: At. Mol. Opt. Phys.* **33** L233
[114] Geltman S 1992 *Phys. Rev.* A **45** 5293
Geltman S 1994 *J. Phys. B: At. Mol. Opt. Phys.* **27** 1497
[115] Mercouris T and Nicolaides C 1999 *J. Phys. B: At. Mol. Opt. Phys.* **32** 2371
[116] Protopapas M, Lappas D G and Knight P L 1997 *Phys. Rev. Lett.* **79** 4550
[117] Patel A, Protopapas M, Lappas D G and Knight P L 1998 *Phys. Rev.* A **58** R2652
[118] Chism W, Choi D I and Reichl L E 2000 *Phys. Rev.* A **61** 054702
[119] Popov A M, Tikhonova O V and Volkova E A 2000 *Laser Phys.* **10** 188

[120] Tikhonova O V, Volkova E A and Skurikhin A V 2002 *Laser Phys.* **12** 424
[121] Grobe R and Eberly J H 1993 *Phys. Rev.* A **47** R1605
[122] Bauer D and Ceccherini 1999 *Phys. Rev.* A **60** 2301
[123] Kulander K C, Schafer K J and Krause J L 1991 *Phys. Rev. Lett.* **66** 2601
[124] Kulander K C, Schafer K J and Krause J L 1992 *Atoms in Intense Laser Fields* ed M Gavrila (New York: Academic) p 247
[125] Tang X and Basile S 1991 *Phys. Rev.* A **44** R1454
[126] Horbatsch M 1991 *Phys. Rev.* A **44** R5346
[127] Latinne O, Joachain C J and Dörr M 1994 *Europhys. Lett.* **26** 333
[128] Lambropoulos P and Tang X 1992 *Atoms in Intense Laser Fields* ed M Gavrila (New York: Academic) p 335
[129] Pont M, Proulx D and Shakeshaft R 1991 *Phys. Rev.* A **44** 4486
[130] Im K, Grobe R and Eberly J H 1994 *Phys. Rev.* A **49** 2853
[131] Huens E and Piraux B 1993 *Phys. Rev.* A **47** 1568
[132] Gajda M, Piraux B and Rzazewski K 1994 *Phys. Rev.* A **50** 2528
[133] Piraux B and Potvliege R M 1998 *Phys. Rev.* A **57** 5009
[134] Bauer J, Plucinski L, Piraux B, Potvliege R, Gajda M and Krzywinski J 2001 *J. Phys. B: At. Mol. Opt. Phys.* **34** 2245
[135] Dondera M, Muller H G and Gavrila M 2002 *Laser Phys.* **12** 415
[136] Dondera M, Muller H G and Gavrila M 2002 *Phys. Rev.* A **65** 031405(R)
[137] Andruszkow J *et al* 2000 *Phys. Rev. Lett.* **85** 3825
[138] Ayvazian V *et al* 2002 *Phys. Rev. Lett.* **88** 104802
[139] Paul P M, Toma E S, Breger P, Mullot G, Augé F, Balcou P, Muller H G and Agostini P 2001 *Science* **292** 1689
[140] Hentschel M, Kienberger R, Spielmann Ch, Reider G A, Milosevic N, Brabec T, Corkum P, Heinzmann U, Drescher M and Krausz F 2001 *Nature* **414** 509
[141] Muller H G 1999 *Laser Phys.* **9** 138
Muller H G 1999 *Phys. Rev. Lett.* **83** 3158
[142] Boca M, Muller H G and Gavrila M, in preparation
[143] Barash D, Orel A E and Baer R 1999 *Phys. Rev.* A **61** 013402
[144] Su Q and Eberly J H 1991 *Phys. Rev.* A **43** 2474
[145] Law C K, Su Q and Eberly J H 1991 *Phys. Rev.* A **44** 7844
[146] Vivirito R M A and Knight P L 1995 *J. Phys. B: At. Mol. Opt. Phys.* **28** 4357
[147] Reed V C, Knight P L and Burnett K 1991 *Phys. Rev. Lett.* **67** 1415
[148] Mittleman M H and Tip A 1984 *J. Phys. B: At. Mol. Phys.* **17** 571
[149] Schiff L 1968 *Quantum Mechanics* 3rd edn (New York: McGraw-Hill) ch 8 section 35
[150] Galindo A and Pascual P 1991 *Quantum Mechanics* (Berlin: Springer) ch 11
[151] Dörr M, Kylstra N J and Potvliege R M 2001 *Laser Phys.* **11** 250
Dörr M, Kylstra N J and Potvliege R M 2001 *Super-Intense Laser–Atom Physics (Proc. SILAP VI)* ed B Piraux and K Rzażewski (Dordrecht: Kluwer) p 305
[152] Cycon H L, Froese R, Kirsch W and Simon B 1987 *Schrödinger Operators* (Berlin: Springer) p 140
[153] Geltman S 1995 *Chem. Phys. Lett.* **237** 286
[154] Leopold J C and Percival I C 1978 *Phys. Rev. Lett.* **41** 944
Leopold J C and Percival I C 1979 *J. Phys. B: At. Mol. Phys.* **12** 709
[155] Percival I C 1977 *Adv. Chem. Phys.* **36** 1
[156] Bayfield J E and Koch P M 1974 *Phys. Rev. Lett.* **33** 258
[157] Abrines R and Percival I C 1966 *Proc. Phys. Soc.* **88** 861
Abrines R and Percival I C 1966 *Proc. Phys. Soc.* **88** 873
[158] Grohmalicki J, Lewenstein M and Rzażewski K 1991 *Phys. Rev. Lett.* **66** 1038
[159] Gajda M, Grohmalicki J, Lewenstein M and Rzażewski K 1992 *Phys. Rev.* A **46** 1638
[160] Rzażewski K, Lewenstein M and Salières P 1994 *Phys. Rev.* A **49** 1196
[161] Ménis T, Taïeb R, Véniard V and Maquet A 1992 *J. Phys. B: At. Mol. Opt. Phys.* **25** L263
[162] Grobe R and Law C K 1991 *Phys. Rev.* A **44** R4114
[163] Bestle J, Akulin V M and Schleich W P 1993 *Phys. Rev.* A **48** 746
[164] Benvenuto F, Casati G and Shepelyansky D L 1992 *Phys. Rev.* A **45** R7670
[165] Benvenuto F, Casati G and Shepelyansky D L 1993 *Phys. Rev.* A **47** R786
[166] Benvenuto F, Casati G and Shepelyansky D L 1994 *Z. Phys.* B **94** 481
[167] Shepelyansky D L 1994 *Phys. Rev.* A **50** 575
[168] Jensen R V and Sundaram B 1990 *Phys. Rev. Lett.* **65** 1964

[169] Sundaram B and Jensen R V 1993 *Phys. Rev.* A **47** 1415
[170] Jensen R V and Sundaram B 1993 *Phys. Rev.* A **47** R778
[171] Watson J B, Keitel C H, Knight P L and Burnett K 1995 *Phys. Rev.* A **52** 4023
Watson J B, Keitel C H, Knight P L and Burnett K 1996 *Phys. Rev.* A **54** 729
[172] Landau L D and Lifshitz E M 1990 *The Classical Theory of Fields* 2nd edn (Oxford: Pergamon) sections 47, 48
[173] Sarachik E S and Schappert G T 1970 *Phys. Rev.* D **1** 2738
[174] Kyrala G A 1987 *J. Opt. Soc. Am.* B **4** 731
[175] Keitel C H and Knight P L 1995 *Phys. Rev.* A **51** 1420
[176] Kylstra N J, Worthington R A, Patel A, Knight P L, Vázquez de Aldana J R and Roso L 2000 *Phys. Rev. Lett.* **85** 1835
[177] Katsouleas T and Mori W B 1993 *Phys. Rev. Lett.* **70** 1561
[178] Krstic P S and Mittleman M H 1990 *Phys. Rev.* A **42** 4037
[179] Krstic P S and Mittleman M H 1992 *Phys. Rev.* A **45** 6514
[180] Ermolaev A M 1998 *J. Phys. B: At. Mol. Opt. Phys.* **31** L65
[181] Faisal F H M and Radożycki T 1993 *Phys. Rev.* A **47** 4464
[182] Radożycki T and Faisal F H M 1993 *Phys. Rev.* A **48** 2407
[183] Potvliege R M 2000 *Laser Phys.* **10** 143
[184] Bugakov A, Pont M and Shakeshaft R 1993 *Phys. Rev.* A **48** R4027
[185] Vázquez de Aldana J R, Kylstra N J, Roso L, Knight P L, Patel A and Worthington R A 2001 *Phys. Rev.* A **64** 013411
[186] Ryabikin M Yu and Sergeev A M 2001 *Laser Phys.* **11** 244
[187] Ryabikin M Yu and Sergeev A M 2000 *Opt. Express* **7** 417
[188] Joachain C J and Kylstra N J 2001 *Laser Phys.* **11** 212
[189] Taïeb R, Véniard V and Maquet A 1998 *Phys. Rev. Lett.* **81** 2882